Zoosyst. Evol. 101 (4) 2025, 1471–1493 | DOI 10.3897/zse.101.155287

A new species of *Hoplias* (Characiformes, Erythrinidae) from the Maranhão State, western Northeast Atlantic basin, Brazil

Karen L. A. Guimarães[1,2*], Juan J. Rosso[3,4*], Mariano González-Castro[3,4], Sarah J. do Nascimento Andrade[2], Pâmella S. Brito[5], Erick C. Guimarães[6], Juan M. Díaz de Astarloa[3,4], Luís R. R. Rodrigues[1,2]

1 *Programa de Pós-Graduação em Biodiversidade e Biotecnologia (REDE BIONORTE), Universidade Federal do Oeste do Pará (UFOPA), Instituto de Saúde Coletiva (ISCO), Santarém, Pará, Brazil*

2 *Laboratório de Genética e Biodiversidade (LGBio), Universidade Federal do Oeste do Pará (UFOPA), Instituto de Ciências da Educação (ICED), Santarém, Pará, Brazil*

3 *Consejo Nacional de Investigaciones Científicas y Técnicas, Buenos Aires, Argentina*

4 *Grupo de Biotaxonomía Morfológica y Molecular de Peces, Instituto de Investigaciones Marinas y Costeras (IIMyC), Facultad de Ciencias Exactas y Naturales, Universidad Nacional de Mar del Plata, CONICET, Funes 3350, (7600) Mar del Plata, Argentina*

5 *Programa de Pós-Graduação em Ciências Ambientais (PPGCAM), Universidade Federal do Maranhão (UFMA), Centro de Ciências de Chapadinha (CCCh), Chapadinha, Maranhão, Brazil*

6 *Programa de Pós-Graduação em Sociedade Natureza e Desenvolvimento (PPGSND), Universidade Federal do Oeste do Pará (UFOPA), Instituto de Biodiversidade e Florestas (IBEF), Santarém, Pará, Brazil*

https://zoobank.org/921E6C1A-EACD-4ECE-9892-C4F20E6D970F

Corresponding author: Juan J. Rosso (plurosso@yahoo.com.ar)

Academic editor: Nicolas Hubert ♦ **Received** 8 April 2025 ♦ **Accepted** 18 July 2025 ♦ **Published** 11 August 2025

Abstract

We describe *Hoplias maranhensis*, a new species within the *Hoplias malabaricus* species-group from Maranhão, northeastern Brazil. The new species is distinguished by a unique combination of morphological, morphometric, and osteological traits, including 14–16 predorsal scales, 37–40 lateral-line scales, 39–40 vertebrae, a straight line formed by the last vertical series of scales at the base of the caudal-fin rays, and a marked ridge on the posterior angular end of the ascending process of the premaxilla. Osteologically, *H. maranhensis* presents the first proximal pterygiophore of the dorsal fin widely bifurcated in a "V"-shaped configuration. *H. maranhensis* also exhibits differences in the articulation pattern of principal caudal-fin rays with lower hypural bones, and postcleithrum 1 exhibits an anterior expansion that is in contact or nearly in contact with postcleithrum 2. The number of predorsal scales (14–16) differentiates *H. maranhensis* from *H. argentinensis* (17–19), *H. microlepis* (17–19), and *H. teres* (18). Likewise, the lateral-line scale count (37–40) and vertebrae count (39–40) distinguish the new species from *H. argentinensis* (41–44; 42–43), *H. teres* (40–41; 42), *H. microlepis* (43–46; 42–43), and *H. mbigua* (41–44; 42). Morphometric traits, such as interlandmark distances 3–5, 1–3, 2–3, 7–10, 8–10, and 9–10, further differentiate *H. maranhensis* from other species in the group. Genetic analysis based on DNA barcoding revealed close affinity with *H. malabaricus* and *H. auri* (3.0% divergence), followed by *H. mbigua* (6.0%) and *H. microlepis* (7.0%). Among the *H. malabaricus* species-group, the most divergent taxa were *H. misionera* and *H. argentinensis* (9.0%). This integrative taxonomic approach supports the recognition of *H. maranhensis* as a distinct taxon.

Key Words

Genetic divergence, geometric morphometry, integrative taxonomy, morphology, osteology, trahira

* These authors contributed equally to this work.

Copyright *Guimarães, K.L.A. et al.* This is an open access article distributed under the terms of the Creative Commons Attribution License (CC BY 4.0), which permits unrestricted use, distribution, and reproduction in any medium, provided the original author and source are credited.

Introduction

The trahiras of the genus *Hoplias* Gill, 1903, are predatory, non-migratory fish species of the family Erythrinidae, which also includes the genera *Hoplerythrinus* Gill, 1896, and *Erythrinus* Scopoli, 1777 (Oyakawa 2003). This family currently hosts 17 valid species (Fricke et al. 2025a) and nine species inquirenda (Toledo-Piza et al. 2024), with *Hoplias* being its most speciose member, comprising a total of 13 valid species (Fricke et al. 2025b). Based on modern integrative taxonomy, new species of *Hoplias* were recently described, considerably expanding its diversity (Azpelicueta et al. 2015; Rosso et al. 2016, 2018; Guimarães et al. 2021a). All of these taxonomic advances have focused on the *Hoplias malabaricus* species-group, a well-populated species complex within the genus, firstly detected by cytogenetics several decades ago (Bertollo 1979; Bertollo et al. 2000) and further supported by various molecular studies (Rosso et al. 2012; Marques et al. 2013; Cardoso et al. 2018; Guimarães et al. 2022).

Recently, a growing database of DNA barcodes (COI mitochondrial gene) has shed light on the cryptic diversity within the *H. malabaricus* species complex, revealing that dozens of mitochondrial lineages previously assigned to *H. malabaricus* could be considered putative new species (Cardoso et al. 2018; Guimarães et al. 2022). At least 22 of these candidate species are recorded in Brazilian drainages outside the La Plata River basin (Guimarães et al. 2022).

Current taxonomic knowledge recognizes only three valid species within the *Hoplias malabaricus* complex throughout the vast Brazilian hydrographic system: *H. malabaricus*, found in the Amazon basin, Western Northeast Atlantic, and São Francisco River basins (Cardoso et al. 2018; Guimarães et al. 2022); *H. misionera*, from a disjunct population recorded in the lower Amazon River (Guimarães et al. 2021b); and *H. auri* (Guimarães et al. 2021a), restricted to the type locality in the Crepori River, Tapajós River basin. Therefore, testing for species validation associated with divergent mitochondrial lineages may be an effective approach for updating *Hoplias* taxonomy.

The Western Northeast Atlantic basin (WNAB) is a large hydrographic province situated between the North and Northeast regions of Brazil. It is structured by six major river basins located primarily in the western part of Maranhão State (approximately 90%), with a smaller portion in northeastern Pará. These basins include the Preguiças, Periá, Munim, Itapecuru, Mearim, Turiaçu, Maracaçumé, and Gurupi rivers, as well as the coastal regions of Maranhão and Pará, which drain into the Northeast Atlantic. While a comprehensive ichthyofaunal survey for the entire WNAB is lacking, studies in Maranhão State have recorded 160 species (Abreu et al. 2019), with a more recent assessment reporting 287 species statewide (Koerber et al. 2023). The Mearim and Itapecuru rivers exhibit the highest species richness, with 154 and 95 species, respectively (Koerber et al. 2023).

Although *Hoplias malabaricus* is currently the only widely recognized trahira species in Maranhão, molecular studies suggest the presence of cryptic diversity within the *H. malabaricus* species-group across major drainages in this region, indicating distinct lineages that have yet to be formally described (Pires et al. 2021).

A new species of *Hoplias*, a member of the *Hoplias malabaricus* species-group, is herein described from the Itapecuru and upper Mearim river basins, two coastal drainages of Maranhão State, northeastern Brazil, based on morphological, osteological, morphometric, and molecular data.

Materials and methods

Ethics statement and specimen preservation

Collections of samples were authorized by the Instituto Chico Mendes de Conservação da Biodiversidade (ICMBio) (Permit nº 77783-1).

Voucher specimens (n = 25) were euthanized by short immersion in an oversaturated eugenol solution, then fixed in 10% formalin for 72 h, rinsed with tap water, and preserved in 70% ethanol (Guimarães et al. 2021a). Type material of the species described herein is deposited in the following ichthyological collections: Fish Collections from the Instituto de Ciências e Tecnologia das Águas, Universidade Federal do Oeste do Pará (UFOPA), and the Instituto de Investigaciones Marinas y Costeras (UNMDP). Acronyms of collections for comparative material follow Fricke and Eschmeyer (2025).

Morphological analysis

Traditional measurements and counts were made on the left side of the body following Fink and Weitzman (1974) *sensu stricto*, with further modifications incorporated by Mattox et al. (2006) and Rosso et al. (2018). A total of 35 counts were recorded (14 for pores, seven for scales, five for teeth and fin rays, three for gill rakers, and one for bands in the anal fin), obtained either visually or by microscope inspection. Vertebral counts, including the anterior four vertebrae of the Weberian apparatus, were performed on radiographed specimens. The counts of the holotype are denoted by an asterisk. Linear body measurements (standard length and 21 additional variables; see Table 1) were taken using a digital caliper to the nearest 0.01 mm.

Osteology

Osteological preparations followed an adapted protocol from Bemis et al. (2004), using dermestid beetles. Initially, specimens underwent external tissue removal with scalpel blades to eliminate scales, muscle, and connective tissue, expediting the drying process. Specimens were then preserved in 70% ethanol for one week to enhance tissue

Table 1. Summary of morphometric data for *Hoplias maranhensis*. Standard length in mm; measurements are expressed as percentages of standard length (1–14) and head length (15–21); n = number, SD = standard deviation. The range values include the holotype.

	Hoplias maranhensis (n = 25)						
		n	Holotype	Mean	Min	Max	SD
	Standard Length	25	260	203.4	116	325	-
1	**Body depth**	20	23.3	22.1	20.1	24.4	1.1
2	**Head length**	25	33.9	31.4	29.2	34.0	0.9
3	**Pectoral-fin length**	25	18.2	17.8	16.1	19.4	0.8
4	**Pelvic-fin length**	25	19.3	19.1	18.0	20.7	0.5
5	**Anal-fin length**	25	19.0	18.6	15.7	20.8	1.2
6	**Dorsal-fin length**	25	33.3	32.0	29.5	34.1	1.2
7	**Dorsal-fin base**	25	20.3	19.0	17.3	21.0	1.0
8	**Anal-fin base**	25	9.3	9.2	7.4	10.6	0.8
9	**Pre-pectoral length**	25	30.1	29.0	26.3	31.0	1.1
10	**Pre-pelvic length**	25	55.5	53.0	48.5	55.7	1.7
11	**Pre-dorsal length**	25	49.9	47.8	45.0	50.0	1.5
12	**Pre-anal length**	23	82.6	81.0	77.0	85.0	2.2
13	**Caudal peduncle depth**	25	13.7	13.0	11.4	13.8	0.6
14	**Caudal peduncle length**	25	13.0	12.7	11.5	14.4	0.7
15	**Snout length**	25	24.8	25.5	22.8	27.5	1.3
16	**Snout width**	25	25.2	23.0	20.4	25.7	1.6
17	**Snout depth**	25	22.1	19.5	16.7	22.3	1.5
18	**Pre-nasal length**	25	16.8	16.0	11.8	18.5	1.5
19	**Orbital diameter**	25	13.6	16.3	13.3	20.1	1.8
20	**Interorbital width**	24	28.2	27.2	22.8	30.7	2.0
21	**Upper jaw length**	24	56.2	54.4	50.1	58.0	1.8

dehydration and prevent fungal growth. Afterward, they were air- and sun-dried for an additional seven days to ensure complete desiccation. Dehydrated specimens were placed in a perforated container within an active dermestid beetle colony. The cleaning process was carefully monitored to prevent excessive disarticulation. Once the bones were free of soft tissue, the specimens were removed, exposed to light to encourage beetle departure, and subsequently frozen to eliminate any remaining beetles. For comparative purposes, osteological preparations were conducted on specimens of *H. maranhensis* (n = 3, UNMDP 5377; UNMDP 5380; UFOPA/LGBIO–CAX23), *H. argentinensis* (n = 3, UNMDP 5388; UNMDP 5389; UNMDP 5390), and *H. auri* (n = 4, UFOPA/LGBIO–CRP71; UFOPA/LGBIO–CRP74; UNMDP 5391; UNMDP 5392). The terminology used to describe osteological elements follows Roberts (1969), consistent with the nomenclature previously adopted by Weitzman (1964).

Landmarks-based morphometric analysis

To characterize body shape variation among different species within the *H. malabaricus* complex, a geometric morphometric approach based on interlandmark distances (Ild) was employed, following González-Castro et al. (2016) and González-Castro and Ghasemzadeh (2016). Twenty-three morphometric variables were recorded as Ild on the left side of the specimens, using a digital caliper with 0.05 mm precision. These variables were derived from 11 anatomical landmarks arranged in a truss network, following the protocol described in Rosso et al. (2018) (Fig. 1). Additional comparative morphometric data for the recently described species *H. mbigua* (n = 14), *H. misionera* (n = 21), *H. argentinensis* (n = 19), and *H. auri* (n = 16), obtained from Guimarães et al. (2021a), were included to compare, characterize, and distinguish the new species described herein.

The morphometric characters were organized by species within the *H. malabaricus* species-group. A normalization technique to scale the data exhibiting allometric growth was applied following Lleonart et al. (2000). Standard length (SL) was taken as the independent variable, while the remaining Ilds were considered dependent variables. In this work, SL_0 represents a reference value (170 mm) to which all individuals were reduced (or amplified). This transformation corrects for allometric effects in morphometric datasets (Lleonart et al. 2000).

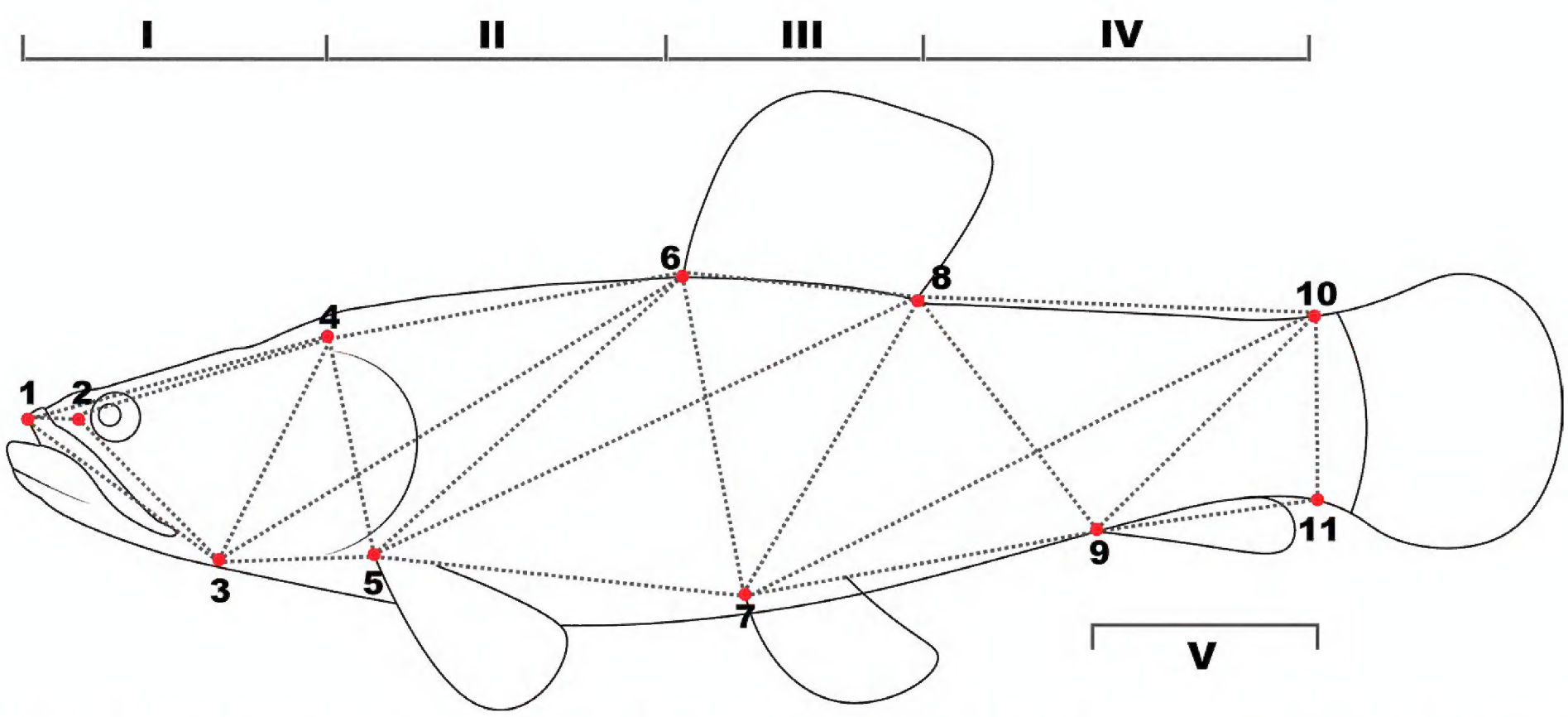

Figure 1. Box-truss showing interlandmark distances based on 11 homologous anatomical landmarks collected in the specimens of the five different species of the *Hoplias malabaricus* species-group analyzed. Box-truss numbers in Roman numerals.

After transformation, a new matrix was constructed containing the corrected values for each species, and a Principal Component Analysis (PCA) was performed using MULTIVARIADO software (Salomón et al. 2004). The principal component scores (PCs) obtained were subjected to cross-validated discriminant analysis (DA) using SPSS v.13.0 in order to build a predictive model of group membership based on the discriminant functions.

Molecular data

Before specimen preservation, tissue samples were collected from the epaxial muscle of 15 individuals, including the type material (see Suppl. material 1 for details), and preserved in absolute ethanol, then frozen at −20 °C until molecular analysis. These analyses used a partial sequence (~620 bp) of the mitochondrial gene cytochrome c oxidase subunit I (COI) as a DNA barcode. Genomic DNA was extracted from the holotype and 14 paratypes using the Salting Out protocol (Aljanabi and Martinez 1997), as adapted by Vitorino et al. (2015). The COI fragment was amplified by polymerase chain reaction (PCR) using FishF1 and FishR1 primers (Ward et al. 2005), and the reactions were performed according to Guimarães et al. (2018). DNA barcode sequences were obtained by capillary sequencing via the dideoxynucleotide (Sanger) method using the ABI PRISM BigDye Terminator v.3 Cycle Sequencing Kit and an ABI3500 Genetic Analyzer (Applied Biosystems).

Sequences were aligned using the ClustalW algorithm (Thompson et al. 1994) implemented in the software BioEdit (Hall 1999). All sequences and specimen metadata were submitted to the Barcode of Life Data System (BOLD; http://www.boldsystems.org) (Ratnasingham and Hebert 2007) and linked to the project "Maranhão Trahiras" (MATRA). To enrich the molecular dataset with comparative material, additional COI sequences were downloaded from BOLD for the following taxa: *H. argentinensis* (n = 15), *H. auri* (n = 15), *H. malabaricus* (n = 20), *H. mbigua* (n = 15), *H. microlepis* (n = 7), *H. misionera* (n = 15), and *H. lacerdae* (n = 2) (see Suppl. material 1).

Molecular species delimitation

Species identification based on DNA barcode sequences was conducted using three delimitation approaches:

1. Barcode Index Number (BIN): Implemented in the BOLD System workbench, the BIN tool uses the RESL (Refined Single Linkage Analysis) algorithm to identify clusters of DNA barcodes. Each cluster receives a unique BIN tag, representing an Operational Taxonomic Unit (OTU) and potential species. A maximum intra-cluster distance threshold of 2.2% is applied; sequences diverging by more than twice this threshold (>4.4%) form new clusters (Ratnasingham and Hebert 2013).
2. Automatic Barcode Gap Discovery (ABGD): It detects discontinuities in pairwise genetic distance distributions (i.e., barcode gaps), serving as evidence of species boundaries (Puillandre et al. 2012). Analyses were performed on the ABGD web platform (http://bioinfo.mnhn.fr/abi/public/abgd/abgdweb.html) using a distance matrix generated in MEGA 11 (Tamura et al. 2021). Parameters included the K80 model, intraspecific divergence ranging from 0.001 to 0.1, and the default barcoding gap setting (X = 1.5).
3. Assemble Species by Automatic Partitioning (ASAP): ASAP partitions single-locus alignments by successively merging sequences into clusters based on barcode gaps and associated probabilities. Analyses were performed on the ASAP web platform (https://bioinfo.mnhn.fr/abi/public/asap), and clusters were ranked using the ASAP score (Puillandre et al. 2021).

As additional evidence for species delimitation, genetic divergences between taxonomically identified species were estimated. A Neighbor-Joining (NJ) tree based on Kimura two-parameter (K2P) distances (Kimura 1980) was constructed in MEGA 11 (Tamura et al. 2021) and visualized using FigTree v1.2.2 (http://tree.bio.ed.ac.uk/software/figtree/).

Results

Hoplias maranhensis Guimarães, Rosso, González-Castro, do Nascimento Andrade, Brito, Guimarães, Díaz de Astarloa & Rodrigues, sp. nov.

https://zoobank.org/CC0CFB0C-0C33-4B78-853E-B806EC0B2A50

Fig. 2, Table 1

Hoplias malabaricus [non Bloch 1794]. Cardoso et al. (2018); Guimarães et al. (2022): (Brazil, Maranhão, Itapecuru River; supported by distinct molecular methods as a putative new undescribed species in the *H. malabaricus* species-group).

Type materials. ***Holotype.*** Brazil • UFOPA-I 001760, 260 mm SL; Maranhão State, Itapecuru basin: Aldeias Altas Municipality, Alagadiço Stream; coordinates: -4.55256, -43.32781; F. Lopes, 10 June 2024; BOLD:ACR9466.

Paratypes. All from Brazil, Maranhão State: Itapecuru Basin: Gonçalves Dias Municipality, Codozinho River: -5.11683, -44.09703, J. O. Sousa, 9 August 2023: • UNMDP 5375, 1, 240 mm SL • UNMDP 5376, 1, 258 mm SL • UNMDP 5377 (osteologic), 1, 280 mm SL • Caxias Municipality, Itapecuru River: -4,87050, -43,36116, A. Lima, 3 December 2021: • UFOPA-I 001757, 4, 161–325 mm SL • UNMDP 5393, 1, 195 mm SL • UNMDP 5378, 1, 180 mm SL • UNMDP 5394, 1, 198 SL • Cajazeira Stream: -4.99417, -43.47751, K. Guimarães, 5 February 2023: • UNMDP 5379, 1, 184 mm SL • UNMDP 5380 (osteologic), 1, 116 mm SL • UFOPA-I 001761, 1, 155 mm SL • Itapecuruzinho Stream: -4,92669, -43,35262, F. Lopes, 10 October 2023: • UNMDP 5381-5384, 4,

Figure 2. *Hoplias maranhensis* sp. nov., holotype, UFOPA-I 001760, 260 mm SL, Alagadiço Stream, Itapecuru River drainage, Brazil.

138-180 mm SL • Ouro Stream: -4.81575, -43.25931, F. Lopes, 9 June 2024: • UFOPA-I 001758, 3, 178–212 mm SL; Aldeias Altas Municipality, Alagadiço Stream: -4.55256, -43.32781, F. Lopes, 10 June 2024: • UFOPA-I 001759, 2, 222–240 mm SL; Gonçalves Dias Municipality, Codozinho River: -5.11683, -44.09703, J. O. Sousa, 9 August 2023: • UFOPA/LGBIO–GCD1, 1, 225 mm SL • UFOPA-I 001762, 1, 258 mm SL.

Non-type specimens. All from Brazil, Maranhão State: Itapecuru Basin: Gonçalves Dias Municipality, Codozinho River: -5.11683, -44.09703, J. O. Sousa, 9 August 2023: • UFOPA/LGBIO–GCD3, 1, 204 mm SL • UFOPA/LGBIO–GCD4, 1, 195 mm SL • UFOPA/LGBIO–GCD8, 1, 283 mm SL; Caxias Municipality, Itapecuru River: Cajazeira Stream: -4.99417, -43.47751, K. Guimarães, 5 February 2023: • UFOPA/LGBIO–CAX8, 1, 100 mm SL • UFOPA/LGBIO–CAX9, 1, 115 mm SL • UFOPA/LGBIO–CAX10, 1, 122 mm SL • UFOPA/LGBIO–CAX11, 1, 95 mm SL • UFOPA/LGBIO–CAX12, 1, 130 mm SL • UFOPA/LGBIO–CAX13, 1, 120 mm SL • UFOPA/LGBIO–CAX14, 1, 99 mm SL • UFOPA/LGBIO–CAX15, 1, 102 mm SL • UFOPA/LGBIO–CAX16, 1, 113 mm SL • UFOPA/LGBIO–CAX19, 1, 80 mm SL • UFOPA/LGBIO–CAX23, 1, 156 mm SL; Peritoró Municipality, Preitoró River: -4,51478, -44,31954, E. C. Guimarães & P. S. Brito, 4 September 2021: • UFOPA/LGBIO–MPI005, 1, 61 mm SL; MEARIM BASIN: Formosa da Serra Negra Municipality, Ribeirão Tamboril: -6.42949, -45.99744, E. C. Guimarães & P. S. Brito, 7 September 2021: • UFOPA/LGBIO–MPI013H1, 1, 51.45 mm SL.

Diagnosis. *Hoplias maranhensis* is distinguished from other species of the *H. malabaricus* species-group by the following combination of characters: 14–16 predorsal scales, 37–40 lateral-line scales, 39–40 vertebrae, 15 branched caudal-fin rays, ii-iii unbranched anal-fin rays, a straight line formed by the last vertical series of scales at the base of the caudal-fin rays, a marked ridge in the posterior angular end of the ascending process of premaxilla, postcleithrum 1 with an anterior expansion and in contact or nearly in contact with an elongated postcleithrum 2, the first proximal pterygiophore of the dorsal fin widely bifurcated, the number of principal caudal-fin rays articulating with lower hypural bones, foramen not in contact with premaxilla border and ascending process of the premaxilla expanded medially and with a dorsoposterior tip.

The number of predorsal scales (14–16), lateral-line scales (37–40), and vertebrae (39–40) distinguishes *H. maranhensis* from *H. argentinensis* (17–19, 41–44, and 42–43, respectively). *H. maranhensis* can be distinguished from *H. microlepis* by predorsal scales (14–16 vs. 17–19), lateral-line scales (43–46), and vertebrae (42–43). Pre-dorsal scales (14–16 vs. 18), lateral-line scales (37–40 vs. 40–41), and vertebrae (39–40 vs. 42) differentiate *H. maranhensis* from *H. teres*. The count of lateral-line scales (37–40) and vertebrae (39–40) distinguishes *H. maranhensis* from *H. mbigua* (41–44 and 42, respectively). *H. maranhensis* is distinguished from *H. auri* by the number of branched caudal-fin rays (15 vs. 12–15), unbranched anal-fin rays (iii–iv vs. ii), lateral-line scales (37–40 vs. 39–40), and vertebrae (39–40 vs. 38–39). *Hoplias maranhensis* differs from *H. misionera* by having a straight line formed by the last vertical series of scales at the base of the caudal-fin rays (*vs.* curved) and two vertical rows of scales on caudal fin (*vs.* four). The shape of the ascending process of the premaxilla distinguishes *H. maranhensis* from *H. malabaricus* (with a marked ridge *vs.* poorly developed) (Fig. 3). *H. maranhensis* also differs from *H. auri* and *H. argentinensis* in some osteological traits: from *H. auri* it differs in postcleithrum 1 (with an anterior expansion vs. no anterior expansion), postcleithrum 2 (more elongated and positioned closer to the base of postcleithrum 1 vs. shorter and more distinctly separated from postcleithrum 1), the first two proximal pterygiophores of the dorsal fin (a bifurcation with a widely divergent "V" shape *vs*. a parallel bifurcation, with a less separation between branches), articulation pattern of principal caudal-fin rays with lower hypural bones (one ray with parahypural, five rays with hypural 1, one ray with hypural 2 vs. two rays with parahypural, three rays with hypural 1 and two rays with hypural 2) (Fig. 4), foramen not in contact with premaxilla border *vs.* foramen in contact; dorsoposterior margin

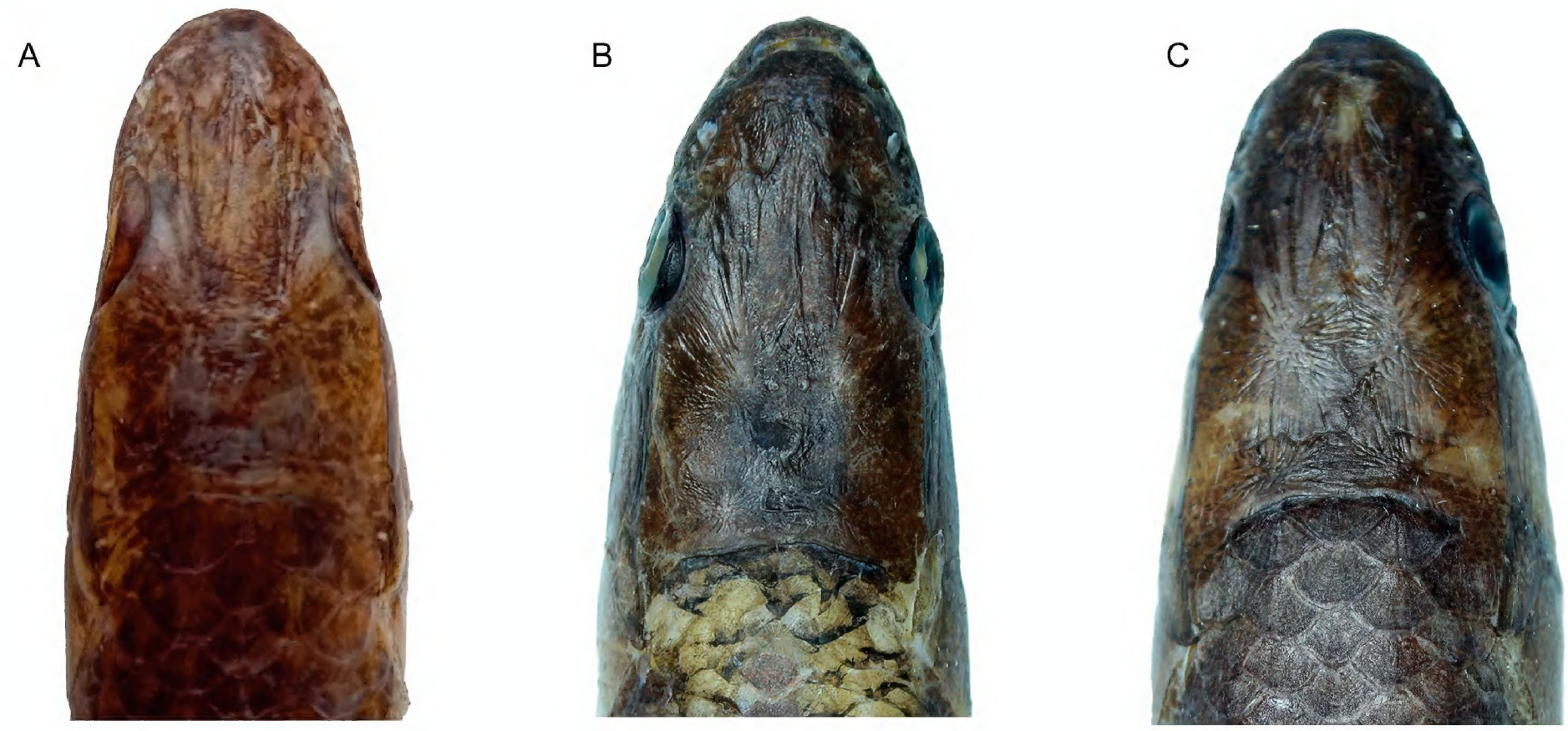

Figure 3. Comparative dorsal view of the head showing the pronounced ridge at the posterior angular end of the ascending process of the premaxilla in *Hoplias maranhensis* vs. slightly developed or no ridge in *Hoplias malabaricus*. *H. maranhensis*: UFOPA/LG-BIO–CAX12, 130 mm SL (**A**); UFOPA-I 001757, 161 mm SL (**B**); UNMDP 5393, 195 mm SL (**C**); and *H. malabaricus*: MNHN-IC-1901-0381, 132 mm SL (collected in Ouanary River, French Guiana, in 1976) (**D**); MHNG 2752.085, 159 mm SL (collected in Saramacca River, Suriname, in 2014) (**E**); MNHN 2003-2527, 204 mm SL (collected in Orapu River, French Guiana, in 2003) (**F**).

of premaxilla projecting medially with an ascending and pointed process vs. not projecting medially and lacking ascending and pointed process) (Fig. 5).

From *H. argentinensis* it differs in postcleithrum 2 (round-shaped and positioned closer to the base of postcleithrum 1 *vs*. a triangular-shaped and more distinctly separated from postcleithrum 1), the first two proximal pterygiophores of the dorsal fin (a bifurcation with a widely divergent "V" shape vs. a parallel bifurcation), and articulation pattern of principal caudal-fin rays with lower hypural bones (one ray articulates with parahypural, five rays with hypural 1, one ray with hypural 2 vs. two rays with parahypural, three or four rays with hypural 1, and one or two rays with hypural 2) (Fig. 3).

Compared to *H. mbigua*, *H. maranhensis* exhibits a straight or slightly convex dorsal head profile (vs. markedly concave) and a longer interorbital width (22.8–30.7%, mean 27.2% vs. 18.5–28.6%, mean 24.3%). Morphometric differences also separate *H. maranhensis* from other species in the group. A longer dorsal-fin base (17.3–21%, mean 19%, vs. 16.2–17.7%, mean 16.9%), a narrower snout (snout width 20.4–25.7%, mean 23%, vs. 29.4–29.5%, mean 29.4%), greater body depth (20.1–24.4%, mean 22.1%, vs. 17–20.6%, mean 18.8%), and greater upper jaw length 54.4 (50.1–58%, mean 54.4%, vs. 50.5–51%, mean 50.7%) distinguish *H. maranhensis* from *H. teres*. *Hoplias maranhensis* differs from *H. microlepis* in snout width (20.4–25.7%, mean 23% vs. 23.6–28.6%, mean 26.8%), pre-nasal length (11.8–18.5%, mean 16.0% vs. 15.4–23.8%, mean 21.4%), pre-dorsal length (45–50%, mean 47.8% vs. 47.7–52.2%, mean 49.8%), and upper jaw length (50.1–58%, mean 54.4% vs. 47.7–53.4%, mean 50.1%). Compared to *H. malabaricus*, *H. maranhensis* differs in having a shorter predorsal

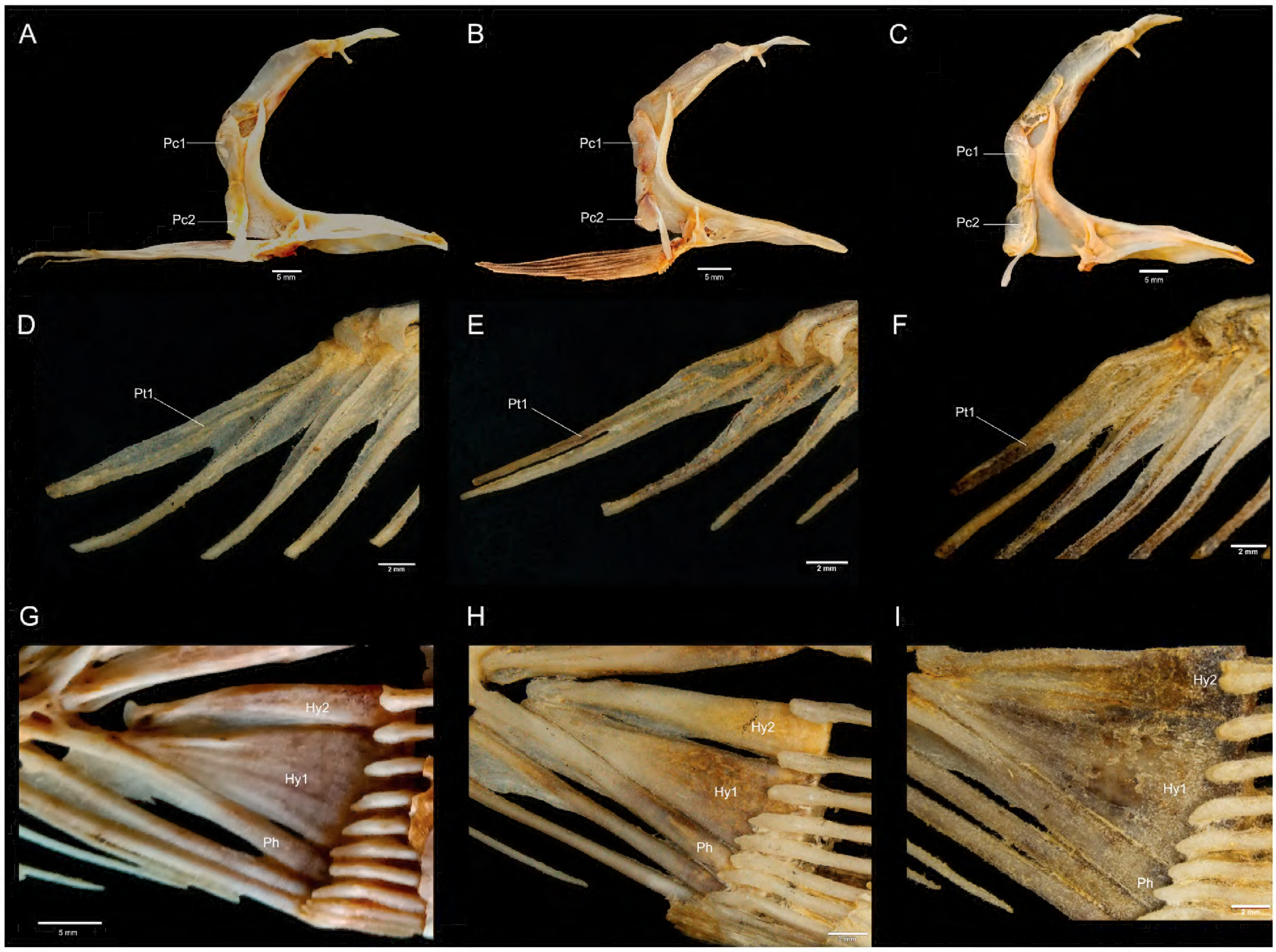

Figure 4. Comparative osteological differences between *Hoplias maranhensis* UNMDP 5377, 280 mm SL (**A, D, G**); *Hoplias auri* UFOPA/LGBIO-CRP71, 235 mm SL (**B**); UNMDP 5391, 211 mm SL (**E**); UFOPA/LGBIO-CRP74, 246 mm SL (**H**); and *Hoplias argentinensis* UNMDP 5390, 287 mm SL (**C, F, I**). **A–C.** Pectoral girdle, showing the postcleithrum 1 (**Pc1**) and postcleithrum 2 (**Pc2**); **D–F.** First proximal pterygiophore (**Pt1**) of the dorsal fin; **G–I.** Articulation pattern of principal caudal-fin rays with lower hypural bones, showing differences in ray connections with parahypural (**Ph**), hypural 1 (**Hy1**), and hypural 2 (**Hy2**).

length (45–50%, mean 47.8%, vs. 48.4–54.4%, mean 50.8%), a longer dorsal-fin (29.5–34.1%, mean 32.0% vs. 28.9–31.1%, mean 32%), a longer dorsal-fin base (17.3–21%, mean 19.0% vs. 15.3–19.2%, mean 17.6%), a longer pre-nasal length (11.8–18.5%, mean 16% vs. 12.5–16.2%, mean 13.8%), and a shorter pre-pelvic length (48.5–55.7%, mean 53% vs. 52.1–58.1%, mean 54.3%). *H. maranhensis* also differs from *H. auri* by a greater body depth (20.1–24.4%, mean 22.1%, vs. 16.2–23%, mean 19.9%), a longer dorsal-fin base (17.3–21%, mean 19.0% vs. 15.1–19.5%, mean 17.5%), and a shorter pre-pelvic length (48.5–55.7%, mean 53% vs. 53.5–58.8%, mean 55.7%) (Fig. 6).

Description. Morphometric data are summarized in Table 1.

Body cylindrical, dorsal profile of head straight or slightly convex. Anterior profile of the head angular to slightly rounded in lateral view, with the greatest body depth at dorsal-fin origin. Dorsal surface of the head with a pronounced ridge at the posterior angular end of the ascending process of the premaxilla, in contact with the mesethmoid medially and the nasal bone laterally (see Fig. 2).

The medial margins of the contralateral dentaries converge at the midline in a V-shaped angle. Both upper and lower lips, fleshy. Anterior nostrils with an incomplete tubular skin flap partially covering the opening, while posterior nostril without fleshy flap and equidistant from the anterior nostril and anterior bony margin of the orbit. Infraorbitals 3 and 4 completely excluded from orbital ring.

Teeth caniniform in both jaws. Premaxilla with a single tooth row containing 9 (1), 10 (23*), or 11 (1) teeth. First two medial teeth large, followed by three to five smaller teeth, ending with two larger canines. First and last canines in this series, the largest. One or two small teeth posterior to last large premaxillary canine, nearly in contact with the first small maxillary tooth. Maxillary row with four to six anterior teeth, progressively increasing in size, followed by 37–46 smaller teeth. External dentary series with one symphyseal tooth, followed by two smaller teeth, another large tooth equal in size to the symphyseal tooth, and largest dentary canine. This is succeeded by three to seven small teeth and a series of six to 11 teeth arranged in a repetitive pattern of one large tooth followed by one, two, or three smaller conical teeth. Internal dentary series with 18–19 very small conical teeth, positioned

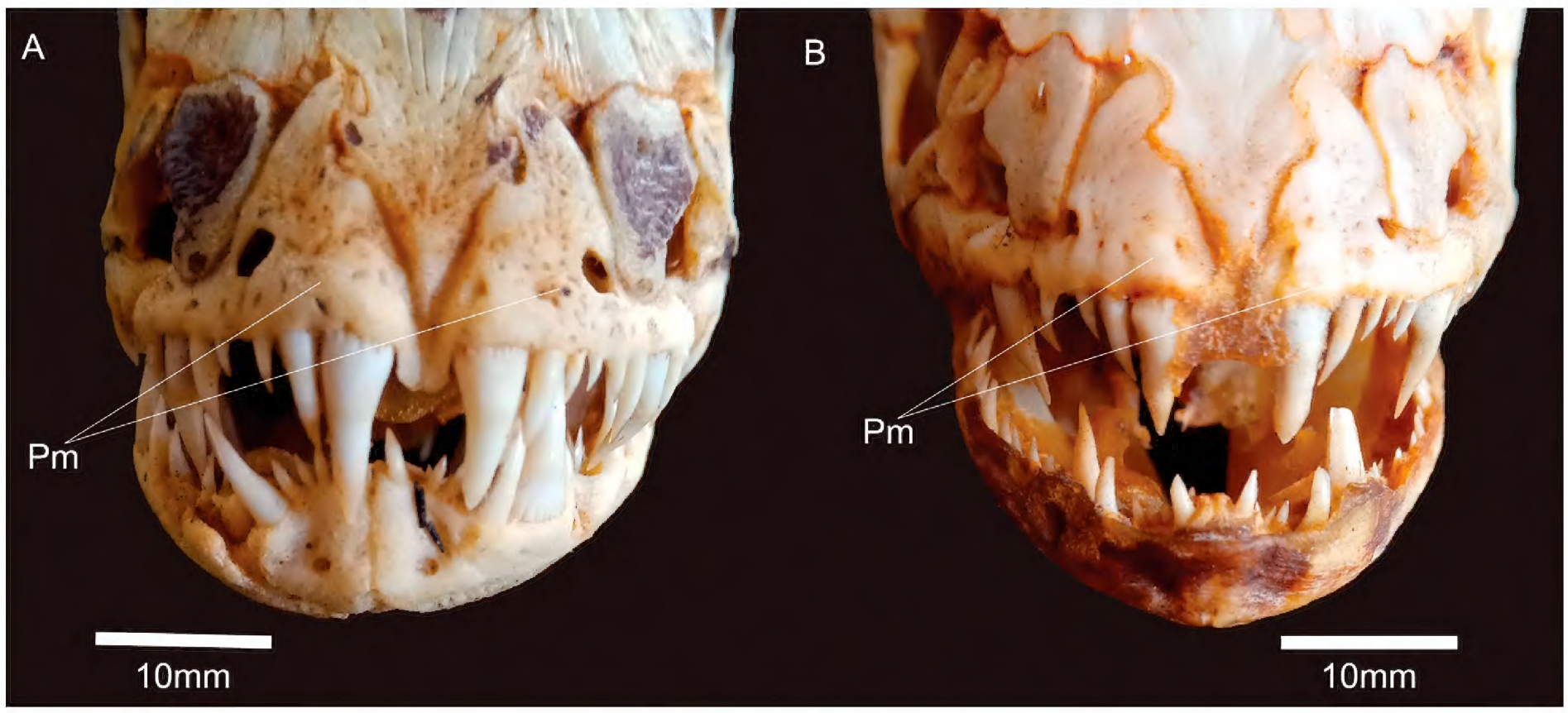

Figure 5. Comparative morphology of the premaxilla in *Hoplias maranhensis* UNMDP 5377, 280 mm SL (**A, C**) and *Hoplias auri* UNMDP 5392, 215 mm SL (**B, D**). **A, B.** Frontal view of the skulls, showing the shape of the premaxillary bone (Pm); **C, D.** Illustration of the premaxilla, highlighting differences in the shape of the ascending process, the medial expansion, and the foramen position.

either immediately posterior or slightly anterior to the last tooth of the external series. Accessory ectopterygoid, a single bone, bearing 10 (2), 11 (2), 12 (7), 13 (6*), 14 (3), or 15 (1) conical teeth along ventrolateral margin.

Dorsal-fin origin positioned at midbody. Dorsal-fin rays ii-11 (4), ii-12 (18*), or ii-13 (3). Anal-fin rays ii-8 in all specimens. Pectoral-fin rays i-12 in all specimens. Pelvic-fin rays i-7 in all specimens. Total number of caudal-fin rays 17 (i-15-i, n = 23). Pectoral-fin tip separated from the pelvic-fin origin by 3–4 scales, while the pelvic-fin tip separated from vertical line through the anus by 2–5 scales.

Predorsal scales 14 (7*), 15 (14), or 16 (1), arranged in irregular series. Lateral line with 37 (3), 38 (10), 39 (9*), or 40 (1) perforated scales, with 1 (6) or 2 (15*) unperforated scales beneath opercular membrane. Two vertical rows present on the caudal-fin rays, similar in size and shape to body scales. Longitudinal scale series between the dorsal-fin origin and the lateral line 5, while those between lateral line and pelvic-fin origin 4 to 5. Caudal peduncle encircled by 20 longitudinal scale series.

First epibranchial with 9–12 gill rakers, first raker somewhat elongated. One angular raker at cartilage. Ceratobranchial with four to five elongated and 10–12 plate-like denticulate rakers. Laterosensory canal along ventral surface of the dentary with four pores, some specimens displaying five pores on one side. Laterosensory canal on preopercle with six pores, while canal along the infraorbitals with 11 pores, distributed as follows: infraorbital 1: 3–4 pores; infraorbital 2: 1–3 pores; infraorbital 3: 1–2 pores; infraorbital 4: 1 pore; infraorbital 5: no pores; infraorbital 6: 3 pores.

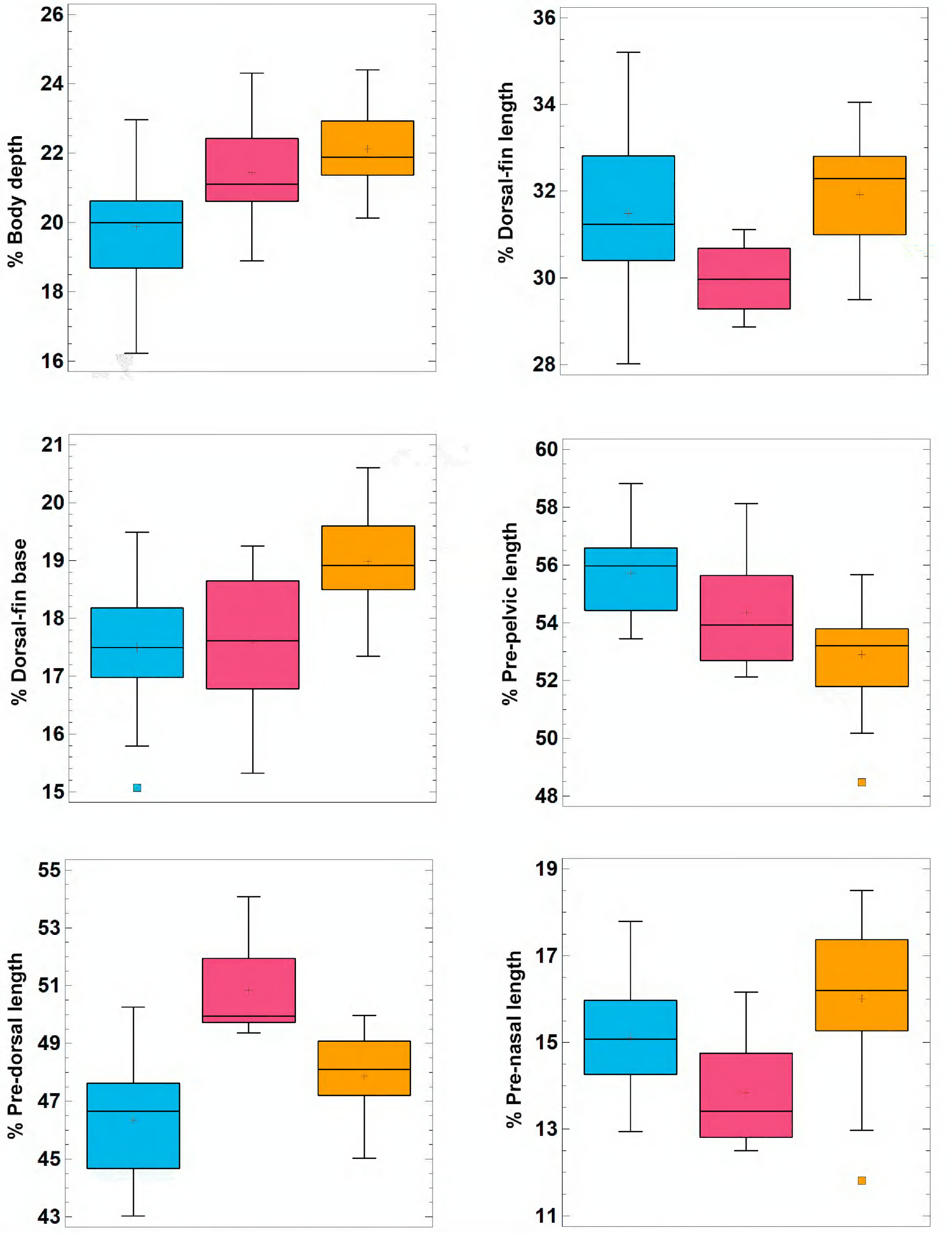

Figure 6. Box plots comparing measurements that differentiate species of the *H. malabaricus* species-group in freshwater of Brazil: *Hoplias auri* (blue), *Hoplias malabaricus* (pink), and *Hoplias maranhensis* (orange). Each box represents the interquartile range, with the horizontal line indicating the median. Whiskers extend to the minimum and maximum values, and outliers are shown as individual points. The red cross marks the mean value for each species.

Laterosensory system on dorsal surface of the head with 11 pores, distributed as follows: nasal: 2 pores; frontal: 4-5 pores; pterotic: 2 pores; and one pore between the parietals at the posterior end of their suture. Supraopercle and extrascapular with following combination of pores: 0–2 (10) or 1–1 (14*). Total vertebrae 39 (n = 6) to 40 (n = 2).

Color in alcohol. Background coloration predominantly black to dark brown, darker along dorsum and close to lateral line. Ventral surface white to pale yellowish, occasionally light brown in some specimens. Scales cycloid, with those on the dorsal half of body with dark-brown melanophores. Scales on ventral half with a dark vertical blotch on their anterior margins; in paler individuals blotch occupies half of scale surface.

Head with variable color patterns: in some specimens, entire head marbled, dark in others. Four distinct dark stripes radiating posteriorly from eye, aligned with infraorbitals 2, 3, and 6, as well as between infraorbitals 4 and 5, with latter the widest. In specimens ≤ 155 mm SL, these stripes are more evident, becoming progressively less conspicuous or almost imperceptible in larger individuals (Fig. 7).

A broad posterodorsal-dark blotch at the junction of opercle and subopercle. Chevron-shaped lateral blotches with vertex directed anteriorly and open arms posteriorly oriented, irregularly spaced, with distance between successive blotches decreasing toward caudal peduncle. These marks less conspicuous or even absent in larger specimens. A dark elliptical or slightly rounded spot on dorsal region of the caudal peduncle, often in contact with dorsal anteroventral branch of last chevron blotch. In specimens < 150 mm SL, dark longitudinal stripe runs along lateral-line scales, covering approximately half of scale series immediately above and below the lateral line. In larger specimens, this stripe becomes indistinct or imperceptible.

Latero-ventral surface of dentaries with transverse brown bands or blotches, occasionally extending to maxilla and lips, or entirely unmarked. Fins light-cream to dark brown, with dark spots across rays and interaxial membranes. Anal fin characterized by larger spots forming irregular dark bands. Pelvic and pectoral fins with a yellowish hue, particularly noticeable in smaller individuals (<150 mm SL). In larger specimens, these fins are darker or with scattered spots across the rays and membranes.

Landmarks-based morphometric analysis. The 23 normalized interlandmark distances, which were analyzed by PCA of the correlation matrix, produced six eigenvalues greater than 1 (5.805, 4.185, 2.831, 1.734, 1.494, and 1.098). The first three PCs explained more than 55% of the variance in the data. Only correlations (between variables and components) higher than 0.5 were taken as significant (Table 2). The first three axes (PC1, PC2, and PC3) of the PCA based on IlD allowed graphic segregation of the five species-groups analyzed.

Table 2. Correlation between interlandmark distances (ILDs) and the first three principal components of the principal component analysis (PCA) of the five species of the *Hoplias malabaricus* species-group analyzed. The most important variables are represented in bold.

	PC1	PC2	PC3
1–2	-0.046	**0.699**	-0.015
1–3	0.327	**0.627**	**-0.581**
1–4	0.087	**0.814**	0.130
2–3	0.327	**0.541**	**-0.654**
3–4	**0.771**	0.343	0.092
3–5	-0.063	0.071	**0.690**
3–6	**0.689**	-0.412	0.271
4–5	**0.715**	0.429	0.228
5–6	**0.840**	-0.403	-0.017
5–7	0.294	0.022	-0.257
5–8	**0.785**	-0.165	0.061
6–7	**0.734**	-0.138	0.102
7–8	**0.776**	-0.270	0.236
7–9	-0.147	**-0.526**	-0.125
7–10	0.333	**-0.502**	**-0.518**
8–9	0.242	-0.381	-0.291
9–10	**0.584**	0.034	-0.459
9–11	0.300	0.175	-0.375
10–11	**0.583**	0.229	-0.020
2–4	0.144	**0.660**	0.251
4–6	0.483	-0.486	0.148
6–8	0.320	0.349	0.183
8–10	-0.363	-0.196	-0.682
Variance %	**25.200**	**18.250**	**12.300**
Cummulaive variance	**25.200**	**43.450**	**55.750**

The multivariate ordination provided by the combination of the first two principal components (PC1–PC2, Fig. 8A, B) allowed graphic segregation of *H. misionera*, *H. auri*, *H. mbigua*, and *H. argentinensis* (first, second, third, and fourth quadrants, respectively) almost without overlapping between them, being *H. maranhensis* located basically in quadrants I and II (PC1–PC2, Fig. 8A, B). However, the PC1–PC3 (Fig. 8C, D) and PC2–PC3 (Fig. 8E, F) axes allowed the graphic segregation of *H. maranhensis* from the remaining four species. In this sense, *H. maranhensis* showed the highest loading for the ILD 3–5 (distance between the anteriormost extreme of interopercle and the origin of pectoral fin). It also displayed the lowest values for ILDs 1–3, 2–3 (variables that indicate the interopercle is located nearer to the tip of the snout), and 9–10, 7–10, 8–10 (which denote a smaller body at the level of the fourth box-truss) (PC1–PC3, Fig. 8C, D;

Figure 7. Progressive reduction of dark stripes radiating from the infraorbitals in *Hoplias maranhensis*. **A.** UNMDP 5380, 116 mm SL; **B.** UFOPA/LGBIO–CAX17, 155 mm SL; **C.** UFOPA-I 001757, 170 mm SL. Scale bar: 10 mm.

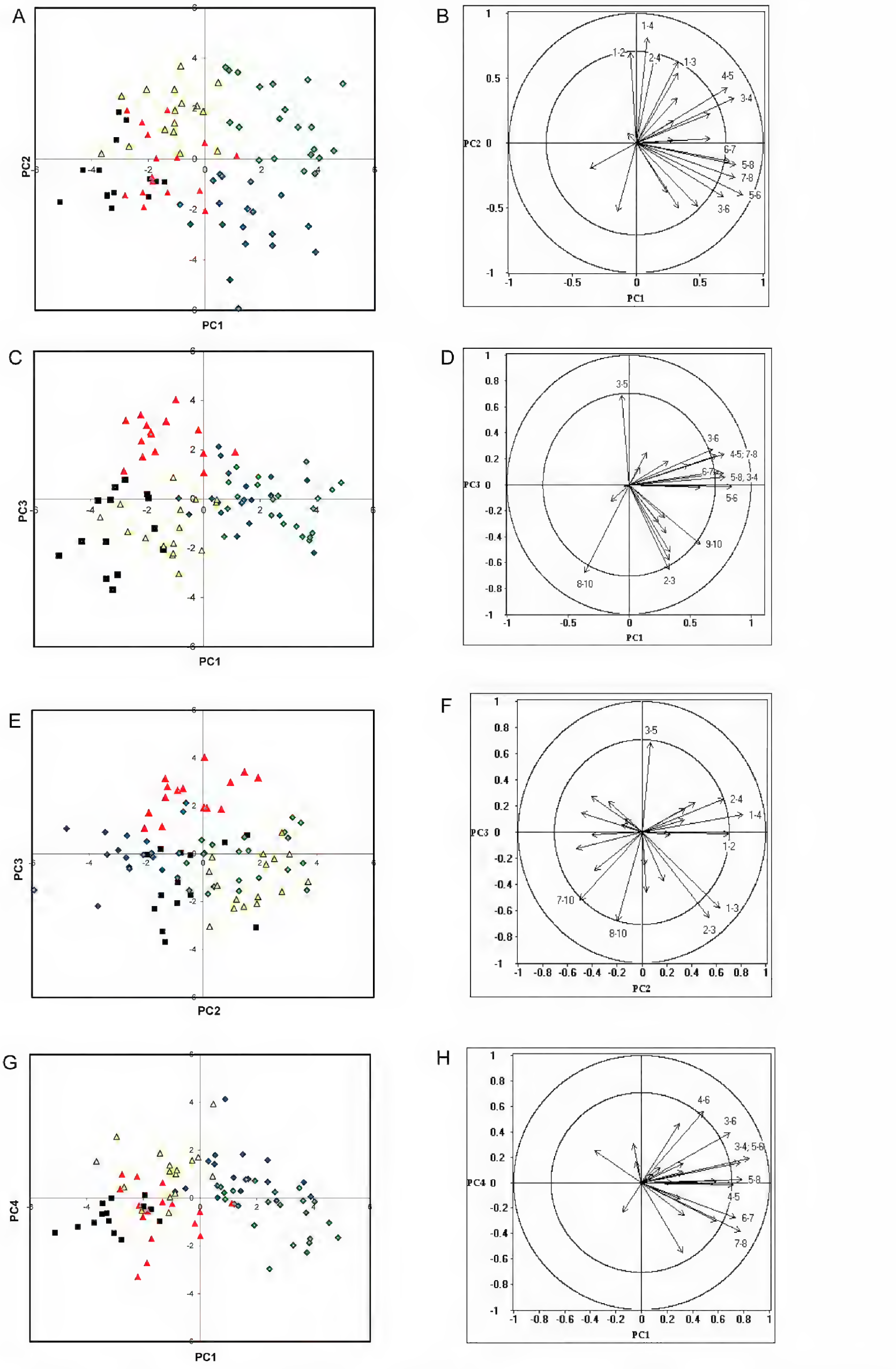

Figure 8. Principal Component Analysis (PCA) of the five species of the *Hoplias malabaricus* species-group. Left: Projections of individuals' scores onto the fourth factorial plane of PCA; PC1-PC2 (**A**); PC1-PC3 (**C**); PC2-PC3 (**E**); PC1-PC4 (**G**). Right: Correlation between interlandmark distances and principal components: PC1-PC2 (**B**); PC1-PC3 (**D**); PC2-PC3 (**F**); PC1-PC4 (**H**). *H. mbigua* (black squares), *H. misionera* (green diamonds), *H. argentinensis* (blue diamonds), *H. auri* (yellow triangles), *H. maranhensis* (red triangles).

PC2–PC3, Fig. 8E, F). In a minor way, *H. maranhensis* showed lower values for ILDs 3–4, 3–6, 4–5, 4–6, 5–6, 5–8, 6–7, and 7–8 (PC1–PC2, Fig. 8A, B; PC1–PC3, Fig. 8C, D; PC1–PC4, Fig. 8G, H), denoting smaller box-trusses II and III, in particular when compared with *H. misionera* and *H. argentinensis*.

H. misionera was basically located on the first quadrant, denoting highest loadings for the 3–4, 4–5, 1–3, 1–4, and 2–4 IlDs (PC1-PC2, Fig. 8) and higher loadings for the 2–3 and 1–2 IlDs (PC2–PC3, Fig. 8E, F). All these ILDs denote a bigger head displayed by *H. misionera* specimens when compared with the other four species-groups analyzed. On the other hand, *H. argentinensis* was located in the fourth quadrant. It was characterized by highest loadings for the 3–6, 5–6, 5–8, 6–7, and 7–8 IlDs (PC1–PC2, Fig. 8A, B), which evidence a robust body at the level of box-trusses II and III, and lower values for the 1–2, 1–4, and 2–4 IlDs (PC2–PC3, Fig. 8E, F).

H. auri was basically located in the second quadrant (PC1–PC2, Fig. 8A, B), being characterized by the highest loadings for 1–2 ILDs, higher loadings for the 1–3, 1–4, 2–3, and 2–4 ILDs, but also 3–4, and 4–5 (in a minor way). These variables represent the head shape, and in particular, 1–2 is in fact correlated to the snout, denoting that *H. auri* possesses a long snout when compared with *H. mbigua*, *H. argentinensis*, and *H. maranhensis*. Moreover, *H. auri* presented lower loadings for the 3–6, 5–6, and 4–6 (minor way) IlDs (variables that represent the relationship between the posterior part of the head and the origin of the dorsal fin) but also lower values for 5–8, 6–7, and 7–8 IlDs (PC1–PC2 Fig. 8A, B and PC1–PC3 Fig. 8C, D) (belonging to the third box-truss and related to the dorsal-fin base and origins of pectoral and ventral fins) (Fig. 1).

Finally, *H. mbigua* showed the highest loadings for the 7–10 and 8–10 IlDs (which represent both the distances between the insertion of the dorsal and anal fins and the first dorsal caudal fin ray insertion) (PC1–PC3, Fig. 8C, D; PC2–PC3, Fig. 8E, F). This species also showed the lowest values for the 3–4 and 4–5 IlDs and lower values for 1–2, 1–3, 2–3, 1–4, and 2–4 but also 5–6, 5–8, 6–7, and 7–8 (PC1–PC2, Fig. 8A, B).

The data corresponding to the 23 PCs of the PCA were employed to perform the DA. The DA for the 86 individuals belonging to the five species analyzed of *Hoplias* produced four significant canonical discrimination functions, where the first two explained 73.8% of the total variance in the data (Wilks lambda = 0.001, $P < 0.000$). Five groups were clearly defined, according to those defined a priori by the PCA, and their centroids and individuals were separated on both the first and second discriminant functions (Fig. 9). The DA correctly classified 100% of the *Hoplias* individuals according to the species-groups defined a priori, whereas the cross-validated analysis correctly classified 93.0% of the fish according to their body shape (Table 3). Accordingly, group misclassifications were scarce, being *H. maranhensis* misclassified as

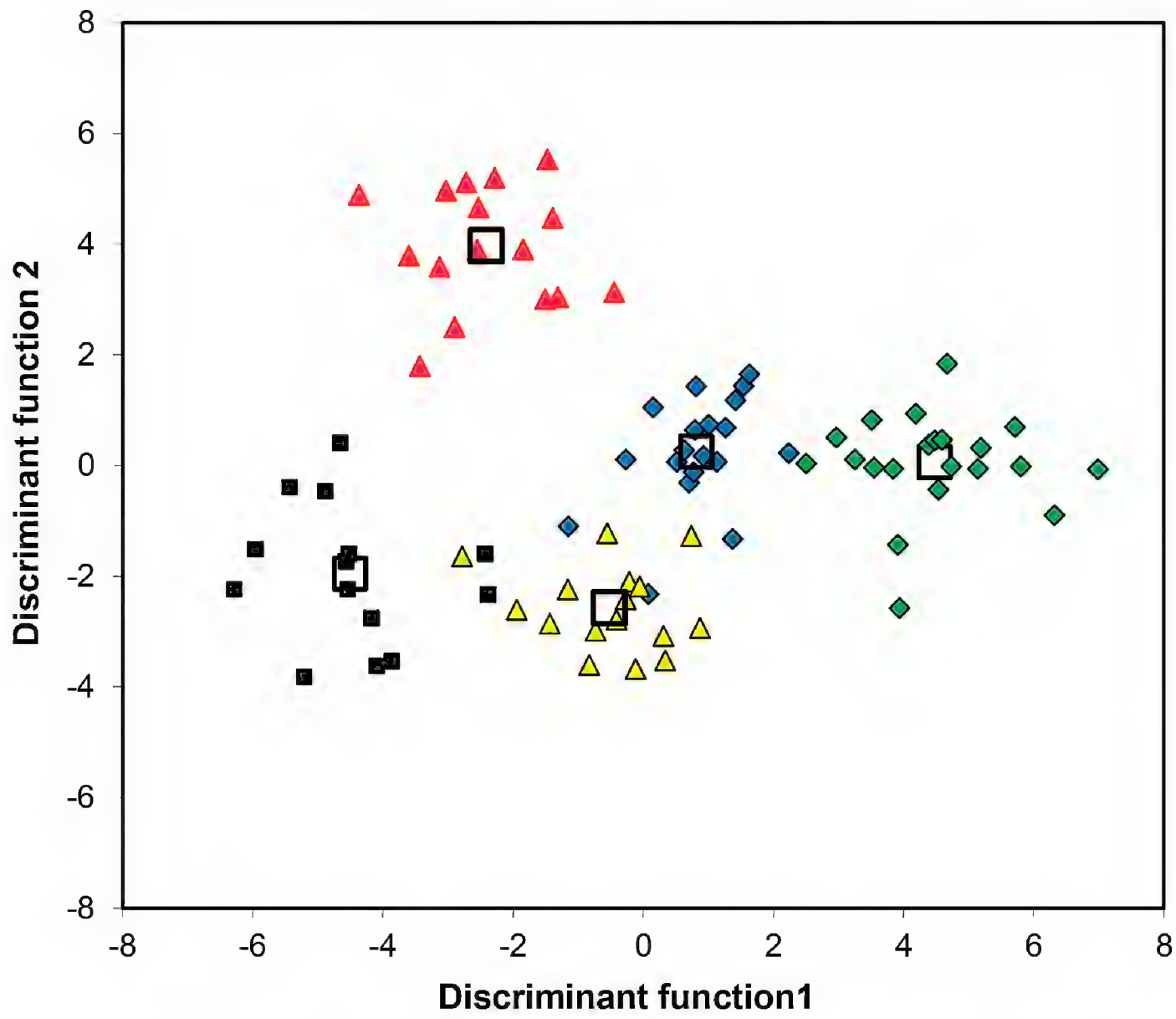

Figure 9. Discriminant analysis of the five species of the *Hoplias malabaricus* species-group: *H. maranhensis* (red triangles), *H. auri* (yellow triangles), *H. argentinensis* (blue diamonds), *H. mbigua* (black squares), and *H. misionera* (green triangles). Black empty squares indicate group centroid location.

Table 3. Cross-validated discriminant analysis based on principal component scores of the interlandmark distances of five species of the *Hoplias malabaricus* species-group. 100.0% of original grouped cases correctly classified; 93.0% of cross-validated grouped cases correctly classified.

			Predicted Group Membership					Total
			H.mbigua	*H. misionera*	*H. argentinensis*	*H. auri*	*H. maranhensis*	
Original	**Count**	*H. mbigua*	14	0	0	0	0	14
		H. misionera	0	21	0	0	0	21
		H. argentinensis	0	0	19	0	0	19
		H. auri	0	0	0	16	0	16
		H. maranhensis	0	0	0	0	16	16
	%	*H. mbigua*	**100.0**	0	0	0	0	100.0
		H. misionera	0	**100.0**	0	0	0	100.0
		H. argentinensis	0	0	**100.0**	0	0	100.0
		H. auri	0	0	0	**100.0**	0	100.0
		H. maranhensis	0	0	0	0	**100.0**	100.0
Cross-validated	**Count**	*H. mbigua*	14	0	0	0	0	14
		H. misionera	0	20	0	0	1	21
		H. argentinensis	0	1	17	1	0	19
		H. auri	0	0	0	16	0	16
		H. maranhensis	1	0	1	1	13	16
	%	*H. mbigua*	**100.0**	0	0	0	0	100.0
		H. misionera	0	**95.2**	0	0	4.8	100.0
		H. argentinensis	0	5.3	**89.5**	5.3	0	100.0
		H. auri	0	0	0	**100.0**	0	100.0
		H. maranhensis	6.3	0	6.3	6.3	**81.3**	100.0

H. mbigua, *H. argentinensis*, and *H. auri* (6.3% in each species-group; Table 3).

Osteological features. *Premaxilla*: bone located at the anteriormost part of the skull, with a dorsal process folded posteroventrally, dorsally narrow and ventrally expanded, bearing teeth along the ventral margin. Bounded posteriorly by the mesethmoid and nasals, laterally by the maxilla, and contacting its counterpart at the snout tip. Approximately triangular in lateral view. A foramen medially, close to but not in contact with premaxilla border. Dorsoposterior margin of premaxilla projecting medially with an ascending and pointed process, accompanied by a marked ridge at its posterior angular (see Fig. 5).

Caudal skeleton. The parahypural does not fully articulate with the hemal spine 38 or 39. The hypural 1 not fully aligned with the length of the parahypural, leaving a small distal gap. The hypural 2 articulates with the hypural 1 but does not extend completely along its length. It does not make contact with the parahypural but may connect anteriorly with the hypural 3. The hypural 3 is the only element articulating with the posterior face of the last centrum and makes full contact with the hypural 4. The hypural 4, in turn, connects with both the urostyle and entirely the hypural 5. The hypural 5 exhibits full contact along its lower margin with the hypural 4, while its upper margin articulates completely with the urostyle and the hypural 6. The hypural 6 fully connects to the hypural 5 along its lower margin and dorsally to both the urostyle and the uroneural bones. The uroneural exhibits full contact with the Urostyle along its upper margin and may also contact the hypural 6 along its lower margin. The epural is entirely in contact with the urostyle and the hemal spine 38 or 39 in its middle region. Hypural bones receive nine principal caudal-fin rays dorsally and eight ventrally. The rays articulate with the hypural bones as follows: the lower unbranched ray articulates with hemal spine 38 or 39; first branched ray is associated with the parahypural; next five branched rays articulate with hypural 1; one with hypural 2; two to three with hypural 3; two to three with hypural 4; two with hypural 5; and one with hypural 6. The latter may be either the last branched ray or the upper unbranched ray, which can articulate with either hypural 6 or the uroneural (Fig. 10).

Pectoral girdle. Pectoral girdle is composed of the posttemporal, supracleithrum, postcleithrum 1–3, mesocoracoid, scapula, cleithrum, and coracoid bones. Posttemporal bifurcated, with a dorsoventrally flattened ascending branch, its anterior portion resembling an arched blade connected to the dorsal surface of the skull. The descending branch, thin and elongated, rod-like in shape. Supracleithrum form the upper portion of the pectoral girdle, an elongated structure, slightly curved at the apex, dorsally articulated with the posttemporal. Ventrally, slightly wider, connected to the cleithrum. Postcleithrum 1, a rounded bone positioned medially to the supracleithrum and laterally to the cleithrum, with a slight anterior expansion. Dorsally located to the ventral end of the supracleithrum. Postcleithrum 2, smaller and laterally narrower than postcleithrum 1, elongated in shape and positioned closer to the base of postcleithrum 1. Connected to the posterior process of the cleithrum and to postcleithrum 3. Postcleithrum 3, slender and narrow, rod-like, positioned below postcleithrum 2, extending to the horizontal line passing through the ventral margin of the coracoid. Scapula a dorsally bifurcated structure at the base of the cleithrum, articulated with the first ray of the pectoral fin. Mesocoracoid a thin, curved bone between the cleithrum and the scapula. Cleithrum dorsally

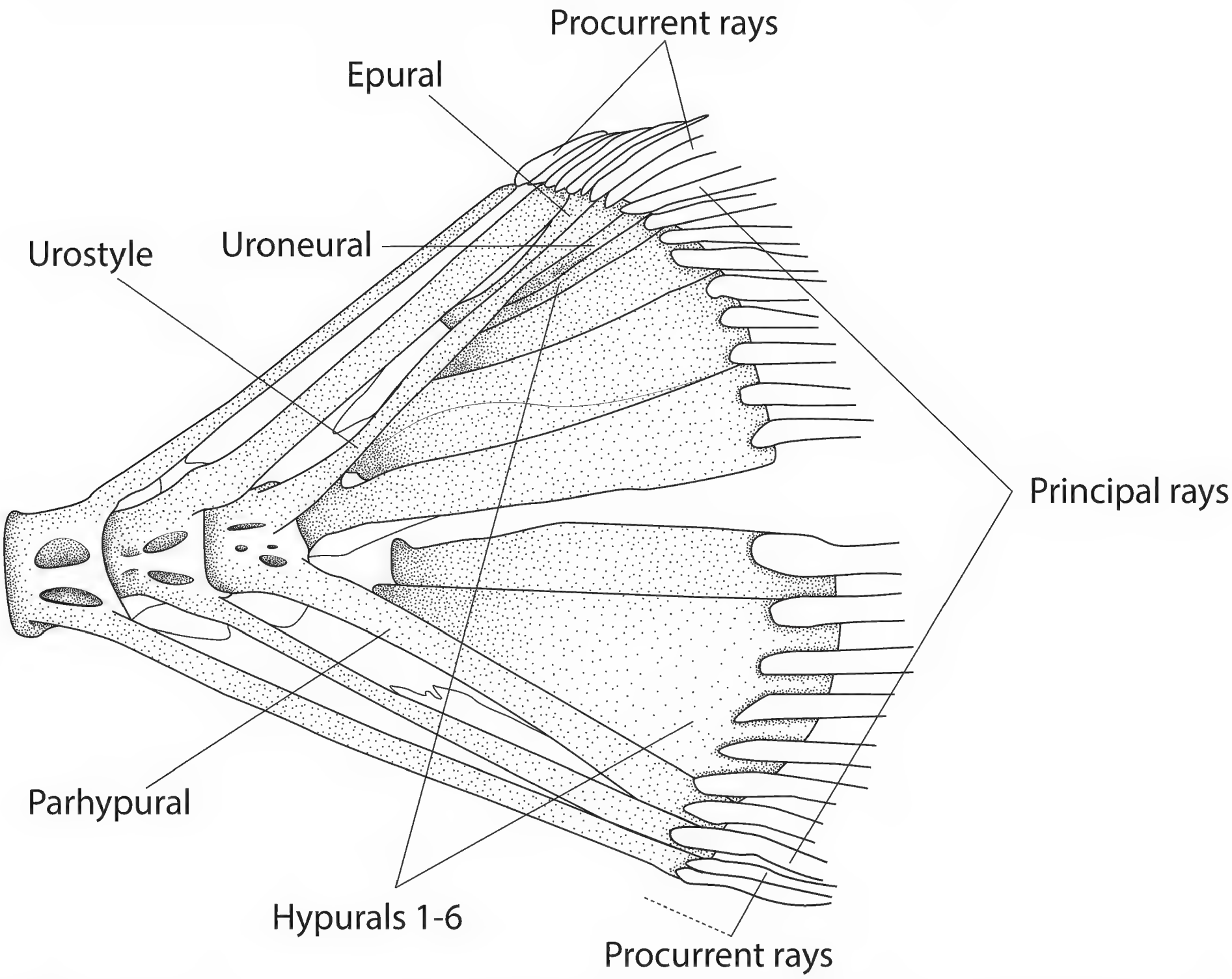

Figure 10. Caudal skeleton illustration of *Hoplias maranhensis*, showing the articulation pattern of principal caudal-fin rays with hypural bones.

articulated with the supracleithrum. An arched bone, broader in the lower portion, gradually narrowing into a curved tip at the apex, directed toward postcleithrum 1. Coracoid anteriorly articulated with the cleithrum. A bone with a triangular outline, a thick base, and a tapered end. Fully connected to the cleithrum, with one foramen in the medial portion (Fig. 11).

Dorsal-fin. A series of 13 distal pterygiophores and 14 proximal pterygiophores. First two proximal pterygiophores fused, and only the second one in contact with a distal pterygiophore. The first proximal pterygiophore (lacking a distal pterygiophore) directly receives the first unbranched dorsal-fin ray. The second proximal pterygiophore in contact with the first distal pterygiophore, and the latter receiving the second unbranched dorsal-fin ray. Distal pterygiophores small, positioned at the junction between the lower end of the fin rays and the proximal pterygiophores. The first two fused proximal pterygiophores, with an anterior bifurcation in a widely divergent "V" shape. Remaining proximal pterygiophores simple, slenderer, and progressively smaller posteriorly (Fig. 12).

Molecular species delimitation. Molecular analyses using the COI gene confirmed the distinctiveness of the new species within the *H. malabaricus* species-group. Species delimitation methods consistently recognized *H. maranhensis* as a genetically distinct lineage. The Barcode Index Number (BIN) algorithm assigned a unique BIN tag (BOLD:ACR9466), indicating clear separation from other *Hoplias* species clusters. Similarly, Automatic Barcode Gap Discovery (ABGD) and Assemble Species by Automatic Partitioning (ASAP) analyses identified a distinct operational taxonomic unit (OTU) for the species, supporting its independent lineage status within the genus (Fig. 13).

Pairwise genetic divergences between *H. maranhensis* and related taxa revealed its closest genetic affinity with *H. malabaricus* (BOLD:AFU2064) and *H. auri* (BOLD:ADL3159), both exhibiting 3.0% divergence. This was followed by *H. mbigua* (BOLD:AAI8239) at 6.0% divergence and *H. microlepis* (BOLD:AAD3629) at 7.0%. Within the *H. malabaricus* species-group, the most divergent taxa from *H. maranhensis* sp. n. were *H. misionera* (BOLD:AAB1732) and *H. argentinensis* (BOLD:AAZ3734), both with 9.0% divergence. The greatest overall genetic distance was observed between *H. maranhensis* sp. n. and the outgroup *H. lacerdae* (BOLD:ABW2258), with a divergence of 17.0% (Table 4). Phylogenetic reconstruction using a Neighbor-Joining

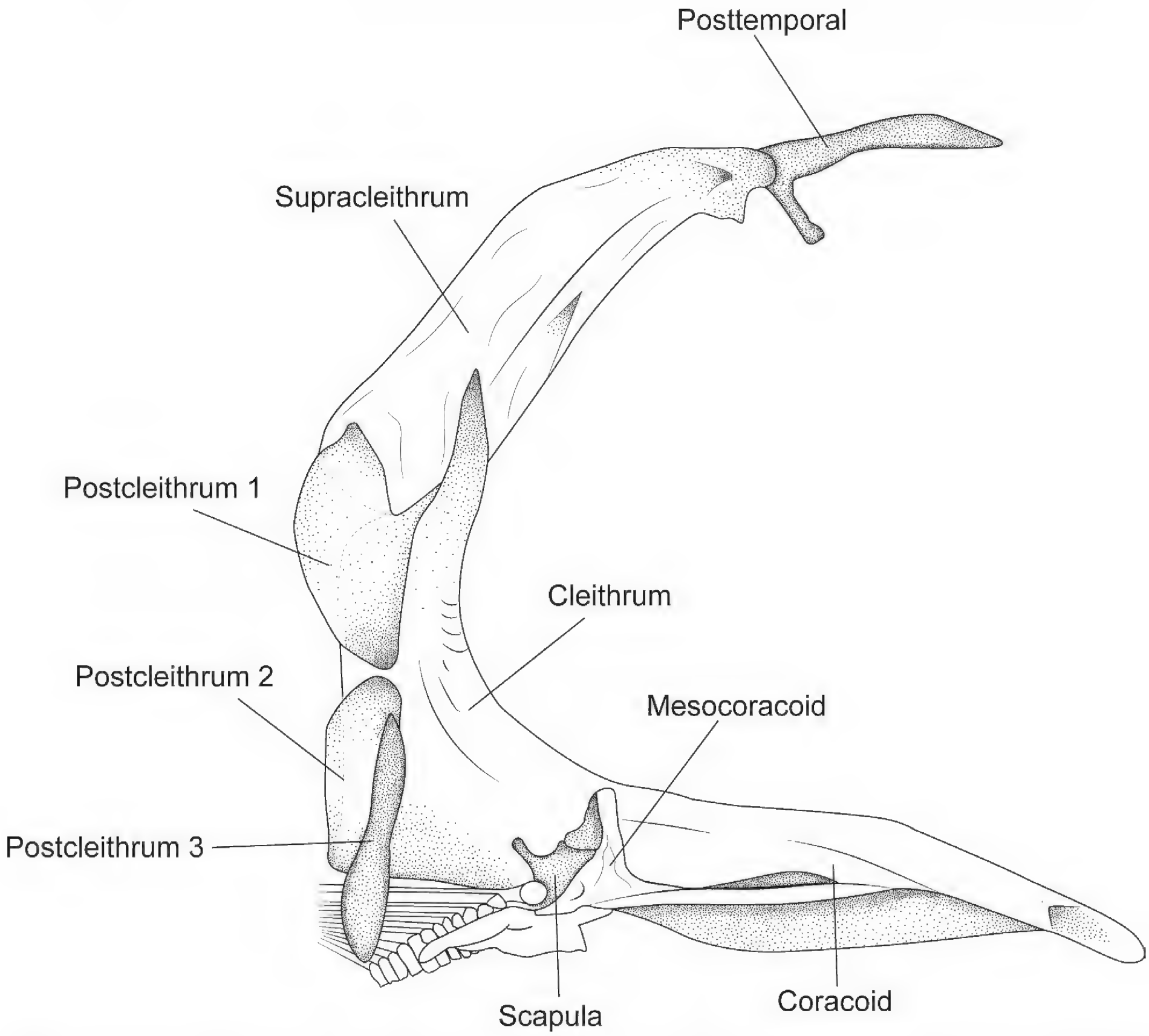

Figure 11. Pectoral girdle illustration of *Hoplias maranhensis*, showing the shape and spatial arrangement of bones, including the anterior expansion of postcleithrum 1, an evaluated informative trait.

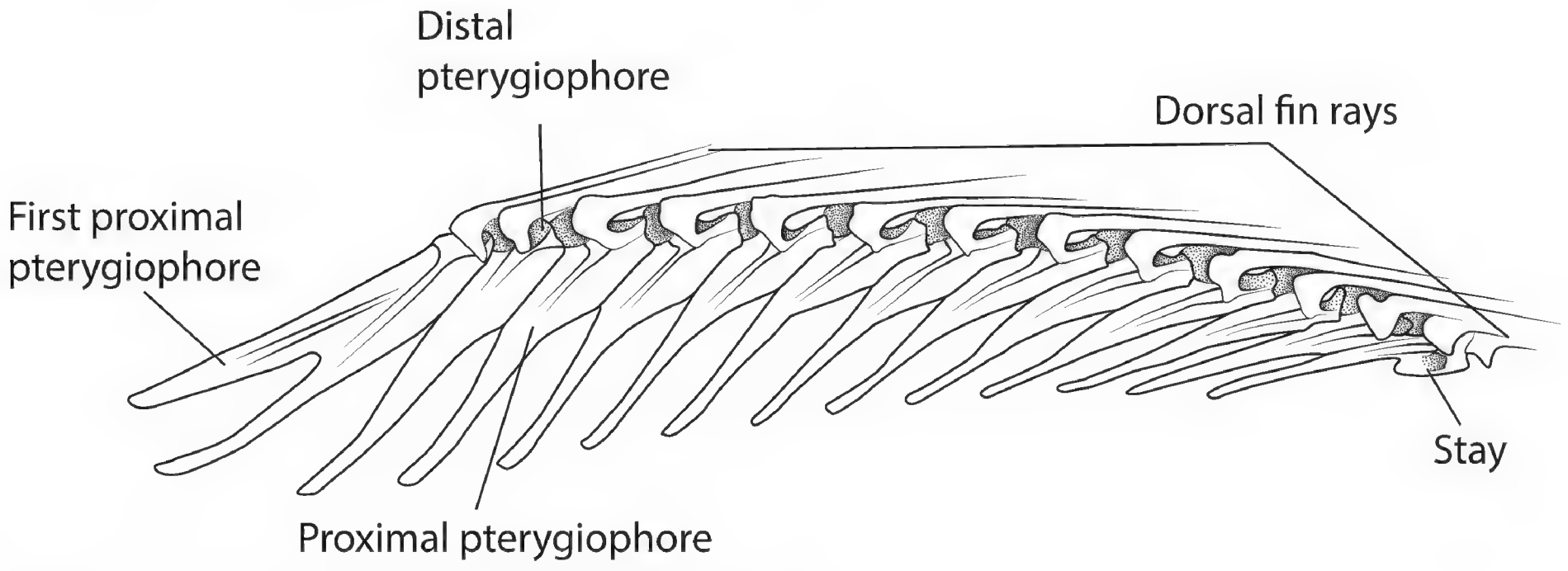

Figure 12. Illustrative dorsal-fin structure of *Hoplias maranhensis*.

(NJ) tree based on Kimura two-parameter (K2P) distances supported these findings, delineating the new species as a well-supported monophyletic clade (Fig. 13).

Etymology. The specific epithet *maranhensis* is related to the place of collection: Maranhão State, in the northeastern, western Atlantic drainages of Brazil.

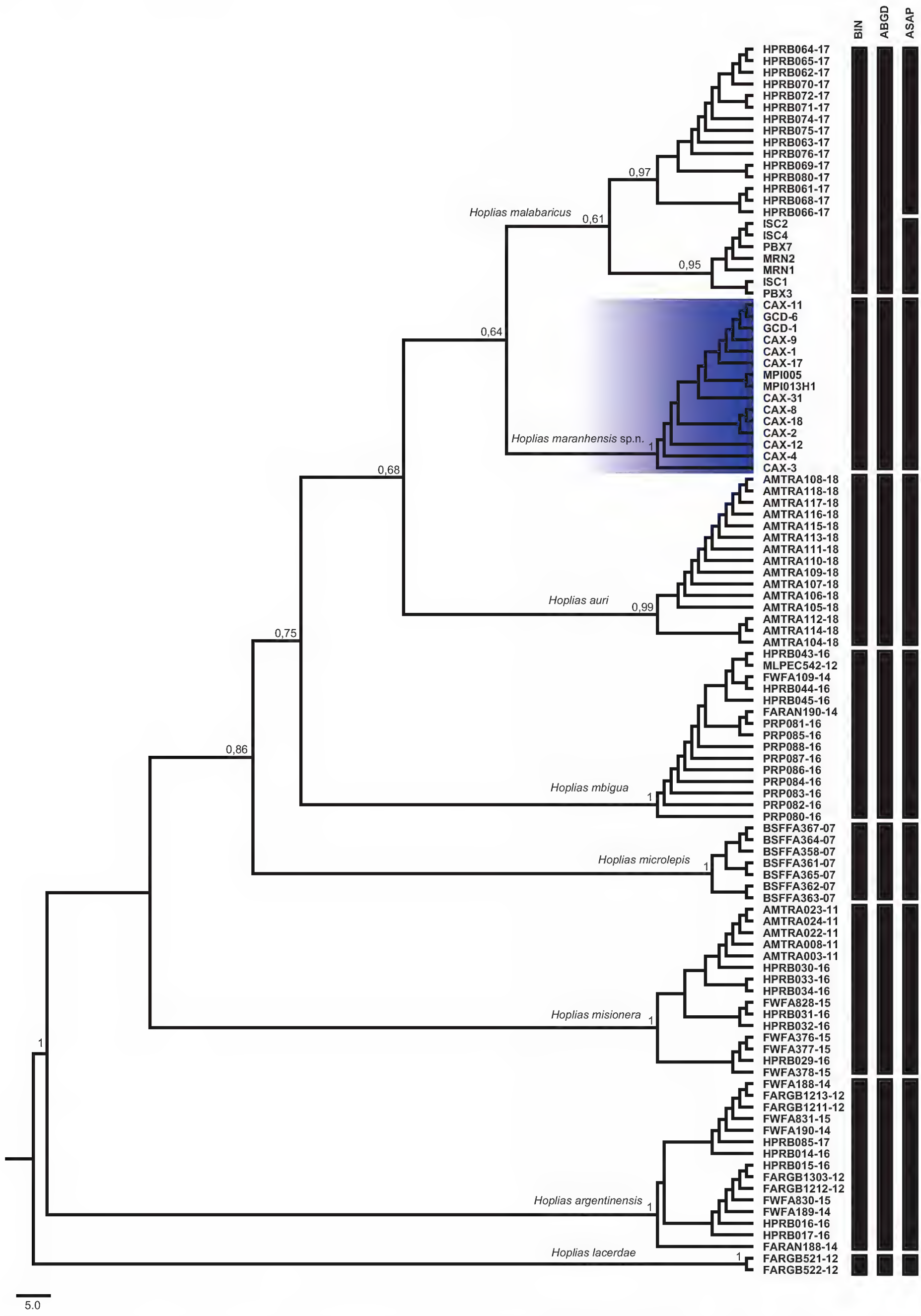

Figure 13. Neighbor-joining tree of *Hoplias maranhensis* and related species of the *H.malabaricus* species-group. Blue indicates the new species. The black lateral bars show the partitions of species delimitation through BIN, ABGD, and ASAP analyses. Values in branches indicate bootstrap values.

Table 4. Mean genetic distances of the Kimura two-parameter (K2P) model between *Hoplias* species.

	Species (BIN)	1	2	3	4	5	6	7	8
1	*Hoplias malabaricus* (BOLD:AFU2064)								
2	*Hoplias auri* (BOLD:ADL3159)	0.03							
3	*Hoplias mbigua* (BOLD:AAI8239)	0.04	0.03						
4	*Hoplias microlepis* (BOLD:AAD3629)	0.06	0.06	0.05					
5	*Hoplias misionera* (BOLD:AAB1732)	0.07	0.07	0.07	0.08				
6	*Hoplias argentinensis* (BOLD:AAZ3734)	0.07	0.08	0.08	0.07	0.08			
7	*Hoplias maranhensis* sp. n. (BOLD:ACR9466)	0.03	0.03	0.06	0.07	0.09	0.09		
8	*Hoplias lacerdae* (BOLD:ABW2258)	0.15	0.15	0.16	0.16	0.14	0.14	0.17	

Distribution. The new species is known from the Western Northeast Atlantic hydrographic region of Maranhão State, predominantly distributed throughout the Itapecuru River basin, including the main river and streams. It also occurs in right-bank tributaries of the Mearim River drainage (Fig. 14).

Conservation issues. The newly described species inhabits river systems in Maranhão State, a region increasingly affected by anthropogenic disturbances, including deforestation, agricultural expansion, and urbanization. These activities contribute to habitat degradation through increased sedimentation and water pollution from agrochemicals and untreated domestic sewage (Bragança 2018, Mataveli et al. 2021, Marengo et al. 2022, Santos et al. 2024). Furthermore, environmental changes can lead to reduced habitat availability, changes in trophic dynamics, and overall declines in freshwater biodiversity (Eastwood et al. 2023). Although trahiras are commonly targeted in subsistence, commercial, and aquaculture in Maranhão State (Guimarães et al. 2021c), the fishing pressure for the fish species is unquantified (Santos et al. 2023). Overfishing, particularly in systems already experiencing environmental degradation, could further threaten population stability. Given these factors, continuous monitoring of habitat integrity, assessment of potential fishery impacts, and implementation of conservation strategies are essential to mitigate eventual threats and ensure the long-term persistence of *H. maranhensis*. Moreover, our sampling program directed to collect specimens of the new species allowed us to record the occurrence of *H. malabaricus* living in sympatry with *H. maranhensis*. This fact poses an additional challenge for any management or conservation strategy intended to be specifically applied to any one of these very similar species.

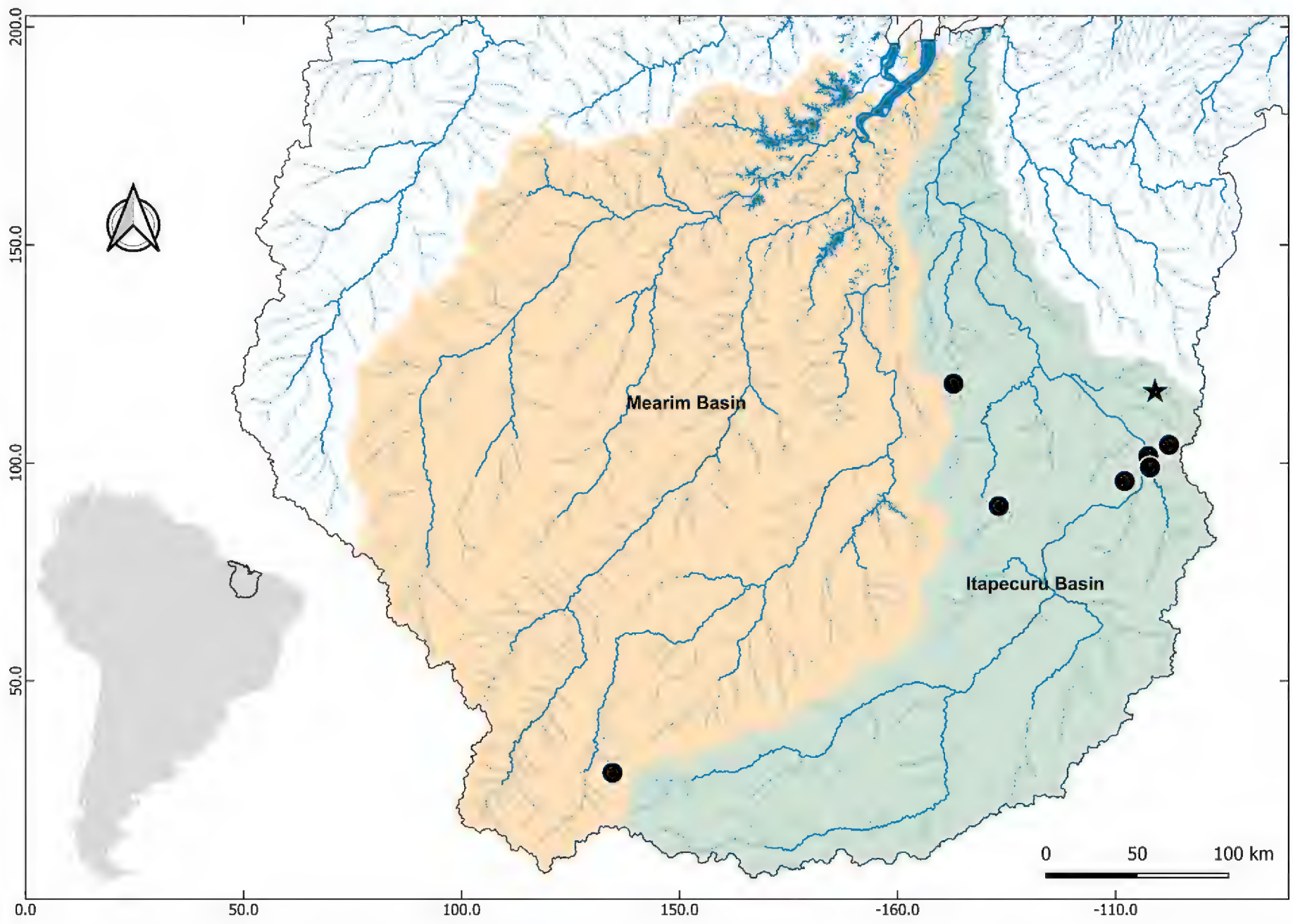

Figure 14. Known distribution of *Hoplias maranhensis* in the Western Northeast Atlantic based on material examined herein (circles indicate paratype localities; star indicates type locality).

Discussion

The *Hoplias malabaricus* species complex has long posed taxonomic challenges due to the high degree of morphological similarity among its members and the plethora of names historically associated with the group. Many of these names were inadequately diagnosed or synonymized without comprehensive revision, contributing to taxonomic instability. Despite the recent description of several new species, these issues persist, underscoring the need for integrative approaches. Particularly, species belonging to the low-count group—which includes *H. malabaricus*, *H. misionera*, and *H. auri* (Rosso et al. 2018; Guimarães et al. 2021a), and now also *H. maranhensis*—are very similar to each other. The overlapping meristic and morphometric traits among these species highlight the limitations of traditional identification methods and emphasize the need for an integrative taxonomic approach. Such approaches have led to a significant increase in the recognized species richness of *Hoplias*, with four new species described, primarily from the La Plata basin (Azpelicueta et al. 2015; Rosso et al. 2016, 2018; Guimarães et al. 2021a). Outside this basin, however, species within the *H. malabaricus* species-group are still frequently identified as *H. malabaricus*, adding uncertainty to knowledge regarding the actual distribution of this species and highlighting the lack of clear morphological taxonomic boundaries for the group. Molecular approaches, particularly DNA barcoding, suggest that *Hoplias* species diversity is severely underestimated (Cardoso et al. 2018; Guimarães et al. 2022). These analyses have been instrumental in distinguishing cryptic diversity, allowing for the detection of genetic divergence among valid and putative species in a scenario lacking taxonomic information for many genetic clades (Marques et al. 2013; Cardoso et al. 2018; Pires et al. 2021; Guimarães et al. 2022).

In this study, a combination of molecular and morphological (morphogeometric, meristic, and osteological) evidence supports the recognition of *H. maranhensis* as an independent evolutionary lineage within the *H. malabaricus* species-group. DNA barcoding analyses revealed clear genetic divergences between *H. maranhensis* and its congeners, with interspecific genetic distances ranging from 3% to 17%, consistent with species-level differentiation in *Hoplias* (Cardoso et al. 2018; Guimarães et al. 2021a, 2022). Additionally, DNA barcode clustering through ABGD and ASAP, as well as the assignment of a unique BIN (BOLD:ACR9466), further reinforces the genetic uniqueness of the taxon and highlights the effectiveness of DNA barcoding in delineating species boundaries within the *H. malabaricus* species-group.

Landmark-based morphometric analyses, including PCA and DA, allowed the characterization and discrimination of *H. maranhensis* from the other four species in the *H. malabaricus* species-group compared in this study. In this sense, this new species was characterized by ILDs belonging to both the head and also the posterior part of its body (fourth box-truss). In particular, *H. maranhensis* showed the highest distance between the anteriormost extreme of interopercle and the origin of the pectoral fin, but also the lowest values for the anterior part of the head (small distances between the tip of the snout/nostril and the interopercle). Moreover, this species displayed a smaller body at the level of the fourth box-truss (a short-tailed species). The DA performed in the present work permitted a clear discrimination of the five species of *Hoplias* analyzed, with 93% of cross-validated grouped cases correctly classified, where *H. maranhensis* showed 81.3% of individuals correctly classified, 89.5% for *H. argentinensis*, 95.2% for *H. misionera*, and 100% for both *H. mbigua* and *H. auri*. This result denotes that landmark-based morphometry is able to delimit species of the *Hoplias malabaricus* species-group on the basis of its body shape, as was previously reported (Rosso et al. 2018; Guimarães et al. 2021a).

The osteology of *Hoplias* has historically been underexplored, with most relevant references relying on the foundational studies of Weitzman (1964) and Roberts (1969), followed by partial contributions on specific structures (e.g., Miquelarena 1984; Vari 1995; Zanata and Vari 2005; Mirande 2010). The osteological comparisons conducted in this study provide additional diagnostic traits, highlighting the importance of skeletal characteristics in resolving species boundaries within *Hoplias*. Among these differences, the structure of the premaxilla is particularly notable in *H. maranhensis*, where the dorsoposterior margin extends medially, forming an ascending and pointed process, whereas in *H. auri*, this projection is absent. Furthermore, in dorsal view, the premaxilla exhibits a more pronounced ascending process in *H. maranhensis* compared to *H. malabaricus*. The premaxilla plays an important role in bite mechanics and may influence feeding strategies, as variations in this structure are often associated with trophic adaptations in fish (Linde et al. 2004; Garita-Alvarado et al. 2021).

Additional differences were observed in structures associated with locomotion, such as elements of the pectoral, dorsal, and caudal fins. Specifically, variations were noted in the shape of postcleithrum 1 and 2 of the pectoral girdle, the configuration of the two first proximal pterygiophores of the dorsal fin, and the articulation pattern of the main caudal fin rays with the lower hypural bones. These traits distinguish *H. maranhensis* from *H. auri* and *H. argentinensis*. While these differences are subtle, they contribute to the osteological evidence supporting the taxonomic delimitation within the *H. malabaricus* species-group.

Genetic data, along with our targeted sampling efforts to collect specimens of the new species, confirm the sympatric occurrence of *Hoplias maranhensis* and *H. malabaricus* in the Mearim and Itapecuru river basins, highlighting important taxonomic and conservation concerns. While *H. malabaricus* has a wide distribution, *H. maranhensis* appears to be more geographically restricted, potentially making it more vulnerable to environmental disturbances. The high morphological similarity between these species may complicate species recognition in

management initiatives, leading to an underestimation of *H. maranhensis* population size and, consequently, inadequate conservation strategies. In this study, comparisons were made exclusively with type material and topotypes of *H. malabaricus* from the Guiana Shield. Genetic evidence revealed high genetic structuring between different populations of *H. malabaricus* across multiple hydrographic basins of South America (Guimarães et al. 2022). In spite of these genetic differences, no morphological study has been conducted to determine whether such structuring is also reflected at the morphological level among genetically analyzed populations. The use of comparative material (both type and topotypes) of *H. malabaricus* limited to the Guiana Shield aimed, therefore, to reduce taxonomic ambiguities that could be introduced by genetically (and perhaps morphologically) distinct populations of *H. malabaricus* from elsewhere in South America. Our results reveal some differences between these two species, particularly in the shape of the ascending process of the premaxilla, which presents a pronounced ridge in *H. maranhensis* but is absent or weakly developed in *H. malabaricus*. Additionally, *H. maranhensis* exhibits a shorter predorsal length (45–50%, mean 47.8%, vs. 48.4–54.4%, mean 50.8%), a longer dorsal-fin (29.5–34.1%, mean 32.0% vs. 28.9–31.1%, mean 32%), a longer dorsal-fin base (17.3–21%, mean 19.0% vs. 15.3–19.2%, mean 17.6%), a longer pre-nasal length (11.8–18.5%, mean 16% vs. 12.5–16.2%, mean 13.8%), and a shorter pre-pelvic length (48.5–55.7%, mean 53% vs. 52.1–58.1%, mean 54.3%). Further research is necessary to determine the actual distribution of *H. malabaricus* and its ecological habits and to establish clearer morphological taxonomic boundaries, which will contribute to a better understanding of the co-distribution patterns between these two species.

Key to the species of the *Hoplias malabaricus* species-group

1 Last vertical series of scales on caudal-fin base curved ..... *Hoplias misionera*.
– Last vertical series of scales on caudal-fin base nearly straight 2
2 Thirty-seven to 40 scales on the lateral line, 38–41 vertebrae (low count group *sensu* Rosso et al. 2018) 3
– Forty to 46 scales on the lateral line, 42–43 vertebrae (high count group *sensu* Rosso et al. 2018) 5
3 Dorsal surface of head with slightly developed, or no notorious ridge ..... *H. malabaricus*
– A marked ridge in the ascending process of premaxilla (Fig. 3) 4
4 Foramen distant from the border of the premaxilla; dorsoposterior margin of premaxilla projecting medially with an ascending and pointed process (Fig. 5) ..... *H. maranhensis* sp. nov.
– Foramen in premaxilla along the lateral border of the premaxilla; dorsoposterior margin of premaxilla not projecting medially and lacking ascending and pointed process (Fig. 5) ..... *H. auri*
5 Twenty-two to 24 scales around caudal peduncle ..... *H. microlepis*
– Twenty scales around caudal peduncle 6
6 Five distinctive transverse bands in the lower jaw, dorsal profile of head concave ..... *H. mbigua*
– No distinctive transverse bands in the lower jaw, dorsal profile of head straight 7
7 Forty-one to 44 scales on the lateral line, snout width less than 25% of head length ..... *H. argentinensis*
– Forty or 41 scales on the lateral line, snout width more than 29% of head length ..... *H. teres*

Comparative material

Hoplias argentinensis: Argentina — 1, **Holotype:** * UNMDP 4417, 1, 302 mm SL. Santa Fe Province, Río Paraná Basin, Río Coronda, 31°50.1'S, 60°51.48'W; 3 Dec 2015; J. J. Rosso, E. Mabragaña & M. González-Castro — 23, **Paratypes:** * **UNMDP 492**, 1, 410 mm SL; Buenos Aires Province, Ascensión, Río Paraná Basin, Río Rojas; Arroyo Santa Cruz; 34°04.2'S, 61°02.6'W; 10 Dec 2010; J. J. Rosso *et al*. 2018 * **UNMDP 502**, 1, 170 mm SL; Buenos Aires Province, Ascensión, Río Paraná Basin, Río Rojas; Arroyo 4 de noviembre; 34°10.2'S, 60°54.1'W; 10 Dec 2010; J. J. Rosso *et al*. 2018 * **UNMDP 503**, 1, 145 mm SL; Buenos Aires Province, Ascensión, Río Paraná Basin, Río Rojas; 34°04.9'S, 61°00.0'W; 10 Dec 2010; J. J. Rosso *et al*. 2018 * **UNMDP 504**, 1, 159 mm SL; Buenos Aires Province, Ascensión, Río Paraná Basin, Río Rojas; 27°28.9'S, 55°46.9'W; 10 Dec 2010; J. J. Rosso *et al*. 2018 **UNMDP 1279**, 1, 240 mm SL; Embalse Salto Grande; 30°56.7'S, 58°01.2'W; 12 Sep 2011; J. J. Rosso & E. Mabragaña * **UNMDP 1370**, 1, 309 mm SL; same locality * **UNMDP 1371**, 1, 265 mm SL; Río Paraná-Guazú, Delta of Río Paraná; 34°02.3'S, 58°35.6'W; 7 Oct 2011; J. J. Rosso *et al*. * **UNMDP 1595**, 1, 98 mm SL; La Plata River, Arroyo Bergara; 32°16.4'S, 59°03.7'W; 9 Sep 2011; J. J. Rosso & E. Mabragaña * **UNMDP 2452**, 1, 202 mm SL, same locality * **UNMDP 2453**, 1, 203 mm SL; Río Paraná basin, Laguna El Pescado; 32°39.3'S, 60°09.4'W; 11 Nov 2012; J. J. Rosso & E. Mabragaña * **UNMDP 2565**, 1, 134 mm SL; Río Paraná Basin, Arroyo Nogoyá; 32°51.1'S, 59°51.7'W; 10 Nov 2012; J. J. Rosso & E. Mabragaña * **UNMDP 2616**, 1, 116 mm SL; Río Uruguay Basin, Arroyo Ayuí; 31°16.4'S, 58°00.3'W; 14 Nov 2012; J. J. Rosso & E. Mabragaña * **UNMDP 3867**, 1, 177 mm SL; Santa Fé Province, Río Paraná Basin, Arroyo Leyes; 31°29.6'S, 60°26.7'W; 25 Apr 2015; J. J. Rosso *et al*. * **UNMDP 4416**, 1, 342 mm SL, same locality * **UNMDP 4423**, 1, 239 mm SL; * **UNMDP 4425**, 1,

203 mm SL; * **UNMDP 4426**, 1, 206 mm SL; * **UNMDP 4427**, 1, 314 mm SL; and * **UNMDP 4428**, 1, 351 mm SL; Río Coronda: collected with the holotype; 31°50.1'S, 60°51.5'W; 3 Dec 2015; J. J. Rosso, E. Mabragaña & M. González-Castro * **UNMDP 4837**, 1, 176 mm SL; Misiones Province, Río Uruguay Basin, Arroyo Fortaleza; 26°41'28"S, 54°12'18"W; 8 Mar 2017; J. J. Rosso *et al.* * **UNMDP 1247**, 1, 45 mm SL; Paraná Basin, Arroyo Las Nutrias; 34°31'35"S, 59°7'29"W * **UNMDP 1248**, 1, 44 mm SL; * **UNMDP 1249**, 1, 55 mm SL. 3, **Non-types: UNMDP 5388**, 1, 220 mm SL; **UNMDP 5389**, 1, 155 mm SL; **UNMDP 5390**, 1, 287 mm SL.

Hoplias auri: Brazil — 1, **Holotype: * UFOPA - I 1353**, 229 mm SL; Brazil, Pará State, Tapajós basin: Crepori River, Itaituba region, Creporizão District, Lago do Sr. Pena, 6°50'1.30"S, 56°50'50.90"W; 21 July 2016; L. Rodrigues, J. Santos, C. Silva, M. Brito — 15, **Paratypes: * UFOPA - I 1353**, 3, 159–202 mm SL; Pará State, Tapajós basin: Crepori River, Itaituba region, Creporizão Village: Lago do Sr. Pena; 6°50'1.30"S, 56°50'50.90"W; 20-21 July 2016; L. Rodrigues, J. Santos, C. Silva, M. Brito * **UNMDP 5206**, 1, 163 mm SL; Lago Creporizão; 6°49'11.56"S, 56°51'4.52"W; 21 July 2016; L. Rodrigues, J. Santos, C. Silva, M. Brito * **UFOPA - I 1355**, 2, 153–154 mm SL; Igarapé da Sra. Maria Brito; 6°49'12.50"S, 56°50'52.80"W; 20 July 2016; L. Rodrigues, J. Santos, C. Silva, M. Brito * **UFOPA - I 1354**, 8, 138–321 mm SL * **UNMDP 5204**, 1, 245 mm SL * **UNMDP 5205**, 1, 194 mm SL, Igarapé Creporizão; 6°49'09"S, 56°51'31"W; 30 April 2008; C. Duarte; 4, **Non-types:** * UFOPA/LGBIO–CRP71, 1, 235 mm SL *; UFOPA/LGBIO–CRP74, 1, 246 mm SL; UNMDP 5391, 1, 211 mm SL*; UNMDP 5392, 1, 215 mm SL.

Hoplias malabaricus: South America — 1, **Lectotype: * ZMB 3515**, 1, 167 mm SL; probably Suriname — 1, **Paralectotypes: * ZMB 33059**, 1, 69 mm SL; probably Suriname. FRENCH GUIANA — 2, **Syntypes of *Macrodon tareira*: * MNHN A-9746**, 1, 93 mm SL; * **MNHN A-9745**, 1, 127 mm SL; 4, **Non-type: * MNHN 1981-0244**, 1, 166 mm SL; * **MNHN 2003-2527**, 2, 166–251 mm SL; * **MNHN 2003-2529**, 2, 141–146.9 mm SL; * **MNHN-IC-1901-0381**, 1, 155 mm TL; * **MHNG 2752.085**, 1, 192 mm TL.

Hoplias mbigua: Argentina — 1, **Holotype: * CI-FML 6763**, 1, 224 mm SL; Misiones: Río Paraná, Nemesio Parma 27°21'23.04"S, 56°1'1.92"W— 17, **Paratypes: * CI-FML 6764**, 2, 224–248 mm SL; Misiones: Río Paraná, Nemesio Parma; collected with the holotype * **LGE-P 314**, 1, 237 mm SL; same locality * **LGE-P 435**, 1, 154 mm SL; Río Paraná, Garupá; 27°27.5'S, 55°48.6'W * **LGE-P 316**, 1, 229 mm SL; Río Paraná, mouth of Arroyo Yabebiry; 27°17.6'S, 55°33.5'W * **LGE-P 317**, 1, 302 mm SL; Río Paraná, Toma de Agua Eriday; 27°29.1'S, 56°40.5'W * **UNMDP 1807**, 1, 67 mm SL; same locality * **UNMDP 2919**, 1, 219 mm SL; La Plata River Basin, Río Paraguay; 26°15.8'S, 58°10.1'W * **UNMDP 4966**, 1, 282 mm SL; Paraná Basin, Río Paraná (Posadas); 27°21'40"S, 55°51'51"W * **CFA-IC34**, 1, 142 mm SL; Laguna Camba Cue Basin, Apipé Grande, Ituzaingó; 27°28'39"S, 56°53'10"W * **CFA-IC3083**, 1, 124 mm SL; Río Paraguay Basin; 26°12'01"S, 58°08'47"W * **CFA-IC722**, 1, 85 mm SL; Cuenca del Paraná Basin, Arroyo San Juan; 27°25'03"S, 55°41'42"W * **CFA-IC4527**, 1, 61 mm SL; Paraná Basin, Arroyo Garupá; 27°29'03"S, 55°47'05"W * **CFA-IC11783**, 1, 305 mm SL; * **CFA-IC4560**, 1, 250 mm SL; Paraná Basin, Arroyo Yabebiry; 27°17'16"S, 55°32'01"W * **CFA-IC40422**, 1, 275 mm SL; * **CFA-IC40403**, 1, 300 mm SL.

Hoplias microlepis: Panamá — 1, **Lectotype: * BMNH 1864.1.26.221**, 1, 278 mm SL; Río Chagres. — 5, **Paralectotypes: * BMNH 1864.1.26.222**, 1, 225 mm SL, same locality * **BMNH 1864.1.26.309**, 1, 176 mm SL; Río Chagres. * **LBP 18503**, 1, 215 mm SL; Atlantic Drainage: Río Llano Sucio. ECUADOR * **BMNH.1860.6.16.128**, 1, 293 mm SL; same locality * **BMNH.1860.6.16.154**, 1, 124 mm SL.

Hoplias misionera: Argentina — 1, **Holotype: * UNMDP 574**, 1, 164 mm SL; Misiones: Río Uruguay Basin: stream tributary to Río Acaraguá; 27°27.8'S, 54°57.1'W — 22, **Paratypes: * UNMDP 1868**, 1, 40 mm SL; same locality * **UNMDP 1950**, 1, 49 mm SL; and * **UNMDP 1951**, 1, 50 mm SL; Formosa: Río Paraguay: Laguna Oca; 26°15.8'S, 58°10.1'W * **UNMDP 1983**, 1, 75 mm SL; Chaco: Río Paraná; 27°47.5'S, 58°49.4'W * **UNMDP 3320**, 1, 174 mm SL; same locality * **UNMDP 3391**, 1, 149 mm SL; and * **UNMDP 3392**, 1, 104 mm SL; same locality as holotype; Misiones: Río Uruguay Basin: stream tributary to Río Acaraguá; 27°27.8'S, 54°57.1'W * **UNMDP 3321**, 1, 142 mm SL; same locality * **UNMDP 3322**, 1, 148 mm SL; Formosa: Río Paraguay: Riacho Saladillo; 26°26.6'S, 58°23.9'W * **UNMDP 3327**, 1, 171 mm SL; same locality * **UNMDP 3328**, 1, 146 mm SL; and * **UNMDP 3329**, 1, 134 mm SL; Formosa: Río Paraguay: Riacho Salado; 26°28.9'S, 58°18.6'W * **UNMDP 3371**, 1, 154 mm SL; same locality * **UNMDP 3376**, 1, 165 mm SL; Formosa: Río Paraguay: Riacho Mbiguá; 26°32.7'S, 58°30.7'W. BRAZIL: * **LBP 32184–32186**, 3, 77–155 mm SL; São Paulo: marginal lagoon: Paraná River * **UNMDP 3865**, 1, 187 mm SL; Paraná Basin, Arroyo Leyes; 31°29.6'S, 60°26.7'W * **UNMDP 3968**, 1, 107 mm SL; Paraná Basin, Laguna Rio Colastiné; 31°37'08"S, 60°35'06"W * **UNMDP 3969**, 1, 99 mm SL; * **UNMDP 3970**, 1, 131 mm SL; Paraná Basin, Río Colastiné; 31°37.4'S, 60°35.1'W * **UNMDP 4424**, 1, 249 mm SL; Paraná Basin, Río Coronda; 31°50.1'S, 60°51.5'W.

Hoplias teres: Venezuela — 2, **Syntypes: * MNHN-4377-1**, 1, 121 mm SL same locality * **MNHN-4377-2**, 1, 116 mm SL; Lago Maracaibo.

Acknowledgments

We are grateful to Tauanny M. A. Lima (UFOPA), who composed the osteological illustrations. This paper is part of K.L.A.G.'s doctoral thesis (PPGBIONORTE-UFOPA). K.L.A.G. received a doctoral scholarship from Coordenação de Aperfeiçoamento de Pessoal de Nível Superior

(PDPG-Amazônia Legal, Programa de Apoio à Pós-Graduação da Amazônia Legal, Grant #88887.630130/2021-00) and a scholarship from PDSE – Programa de Doutorado Sanduíche no Exterior (Grant #88881.846231/2023-01). We would like to express our gratitude to the fishermen who supported the sampling efforts (Jurandir Sousa, Afonso Lima, and Francisco Lopes) and to those who provided logistical support (Tânia, Gilmar, Laura, Kellyane, Diego, and Patrícia). We are also indebted to Yamila P. Cardoso for sharing with us the photograph of the specimen MHNG 2752.085 deposited at the Museum of Natural History in Geneva. This paper benefited from the valuable suggestions of three reviewers: George Mattox, Kleber Mathubara, and one anonymous reviewer.

References

Abreu JMS, Craig JM, Albert JS, Piorski NM (2019) Historical biogeography of fishes from coastal basins of Maranhão State, northeastern Brazil. Neotropical Ichthyology 17: e180156. https://doi.org/10.1590/1982-0224-20180156

Aljanabi SM, Martinez I (1997) Universal and rapid salt-extraction of high quality genomic DNA for PCR-based techniques. Nucleic Acids Research 25(22): 4692–4693. https://doi.org/10.1093/nar/25.22.4692

Azpelicueta M, Benitez M, Aichino D, Mendez D (2015) A new species of the genus *Hoplias* (Characiformes, Erythrinidae), a tararira from the lower Paraná River, in Misiones, Argentina. Acta Zoológica Lilloana 59: 71–82.

Bemis WE, Hilton EJ, Brown B, Arrindell R, Richmond AM, Little CD, Grande L, Forey PL, Nelson GJ (2004) Methods for Preparing Dry, Partially Articulated Skeletons of Osteichthyans, with Notes on Making Ridewood Dissections of the Cranial Skeleton. Copeia 2004(3): 603–609. https://doi.org/10.1643/CI-03-054R1

Bertollo LAC (1979) Karyotypic studies of two allopatric populations of the genus Hoplias (Pisces, Erythrinidae) 2: 17–37.

Bertollo LAC, Born GG, Dergam JA, Fenocchio AS, Moreira-Filho O (2000) A biodiversity approach in the neotropical Erythrinidae fish, *Hoplias malabaricus*. Karyotypic survey, geographic distribution of cytotypes and cytotaxonomic considerations. Chromosome Research 8(7): 603–613. https://doi.org/10.1023/A:1009233907558

Bragança A (2018) The Economic Consequences of the Agricultural Expansion in Matopiba. Revista Brasileira de Economia 72(2): 161–185. https://doi.org/10.5935/0034-7140.20180008

Cardoso YP, Rosso JJ, Mabragaña E, González-Castro M, Delpiani M, Avigliano E, Bogan S, Covain R, Schenone NF, de Astarloa JMD (2018) A continental-wide molecular approach unraveling mtDNA diversity and geographic distribution of the Neotropical genus *Hoplias*. PLoS ONE 13(8): e0202024. https://doi.org/10.1371/journal.pone.0202024

Eastwood N, Zhou J, Derelle R, Abdallah MA-E, Stubbings WA, Jia Y, Crawford SE, Davidson TA, Colbourne JK, Creer S, Bik H, Hollert H, Orsini L (2023) 100 years of anthropogenic impact causes changes in freshwater functional biodiversity. eLife 12: RP86576. https://doi.org/10.7554/eLife.86576

Fink WL, Weitzman SH (1974) The so-called cheirodontin fishes of Central America with descriptions of two new species (Pisces, Characidae). http://repository.si.edu/xmlui/handle/10088/5121 [May 18, 2023]

Fricke R, Eschmeyer WN (2025) Guide to Fish Collections. Eschmeyer's Catalog of Fishes. http://researcharchive.calacademy.org/research/ichthyology/catalog/collections.asp [February 28, 2025]

Fricke R, Eschmeyer WN, Fong JD (2025a) Genera/Species by Family/Subfamily. Eschmeyer's Catalog of Fishes. http://researcharchive.calacademy.org/research/ichthyology/catalog/SpeciesByFamily.asp [February 28, 2025]

Fricke R, Eschmeyer WN, van der Laan R (2025b) Genera, Species, References. Eschmeyer's Catalog of Fishes. http://researcharchive.calacademy.org/research/ichthyology/catalog/fishcatmain.asp [February 28, 2025]

Garita-Alvarado CA, Garduño-Sánchez M, Barluenga M, Ornelas-García CP (2021) Genetic and ecomorphological divergence between sympatric *Astyanax* morphs from Central America. https://doi.org/10.1101/2021.04.29.442001

González-Castro M, Ghasemzadeh J (2016) Biology, Ecology and Culture of Grey Mullets (Mugilidae) Morphology and Morphometry Based Taxonomy of Mugilidae. CRC Press - Taylor & Francis Group. https://ri.conicet.gov.ar/handle/11336/132263 [May 17, 2023]

González-Castro M, Rosso JJ, Mabragaña E, Díaz de Astarloa JM (2016) Surfing among species, populations and morphotypes: Inferring boundaries between two species of new world silversides (Atherinopsidae). Comptes Rendus Biologies 339(1): 10–23. https://doi.org/10.1016/j.crvi.2015.11.004

Guimarães KLA, de Sousa MPA, Ribeiro FRV, Porto JIR, Rodrigues LRR (2018) DNA barcoding of fish fauna from low order streams of Tapajós River basin. PLoS ONE 13(12): e0209430. https://doi.org/10.1371/journal.pone.0209430

Guimarães KLA, Rosso JJ, González-Castro M, Souza MFB, Díaz de Astarloa JM, Rodrigues LRR (2021a) A new species of *Hoplias malabaricus* species complex (Characiformes, Erythrinidae) from the Crepori River, Amazon basin, Brazil. Journal of Fish Biology 100(2): 425–443. https://doi.org/10.1111/jfb.14953

Guimarães KLA, Rosso JJ, Souza MFB, Díaz de Astarloa JM, Rodrigues LRR (2021b) Integrative taxonomy reveals disjunct distribution and first record of *Hoplias misionera* (Characiformes, Erythrinidae) in the Amazon River basin: Morphological, DNA barcoding and cytogenetic considerations. Neotropical Ichthyology 19(2): e200110. https://doi.org/10.1590/1982-0224-2020-0110

Guimarães EC, Brito PS, Santos JP, Anjos MR, Andrade MC, Lopes DFC, Ramos TPA, Costa SYL, Guimarães KLA, Rodrigues LRR, Carvalho-Costa LF, Ferreira LM, Silva SGB, Santos J de RC, Dias LJB da S (2021c) Peixes comerciais do estado do Maranhão. Guimarães EC, Brito PS de, Santos JP, dos Anjos MR, Andrade MC, Ramos TPA, Carvalho-Costa LF, Lopes DFC (Eds) IMESC, São Luís, MA, 69 pp.

Guimarães KLA, Lima MP, Santana DJ, de Souza MFB, Barbosa RS, Rodrigues LRR (2022) DNA barcoding and phylogeography of the *Hoplias malabaricus* species complex. Scientific Reports 12(1): 5288. https://doi.org/10.1038/s41598-022-09121-z

Hall T (1999) BIOEDIT: A user-friendly biological sequence alignment editor and analysis program for windows 95/98/ NT., 95–98.

Kimura M (1980) A simple method for estimating evolutionary rates of base substitutions through comparative studies of nucleotide sequences. Journal of Molecular Evolution 16(2): 111–120. https://doi.org/10.1007/BF01731581

Koerber S, Guimarães EC, Brito PS de, Oliveira RF de, Ottoni FP (2023) CLOFFBR-MA - update 1 - supplement to Checklist of the freshwater fishes of Maranhão, Brazil. Ichthyological Contributions of PecesCriollos: 1–13. https://doi.org/10.5281/ZENODO.11558473

Linde M, Palmer M, Gómez-Zurita J (2004) Differential correlates of diet and phylogeny on the shape of the premaxilla and anterior tooth in sparid fishes (Perciformes, Sparidae). Journal of Evolutionary Biology 17(5): 941–952. https://doi.org/10.1111/j.1420-9101.2004.00763.x

Lleonart J, Salat J, Torres GJ (2000) Removing Allometric Effects of Body Size in Morphological Analysis. Journal of Theoretical Biology 205(1): 85–93. https://doi.org/10.1006/jtbi.2000.2043

Marengo JA, Jimenez JC, Espinoza J-C, Cunha AP, Aragão LEO (2022) Increased climate pressure on the agricultural frontier in the Eastern Amazonia–Cerrado transition zone. Scientific Reports 12(1): 457. https://doi.org/10.1038/s41598-021-04241-4

Marques DF, dos Santos FA, da Silva SS, Sampaio I, Rodrigues LRR (2013) Cytogenetic and DNA barcoding reveals high divergence within the trahira, *Hoplias malabaricus* (Characiformes, Erythrinidae) from the lower Amazon River. Neotropical Ichthyology 11(2): 459–466. https://doi.org/10.1590/S1679-62252013000200015

Mataveli GAV, de Oliveira G, Seixas HT, Pereira G, Stark SC, Gatti LV, Basso LS, Tejada G, Cassol HLG, Anderson LO, Aragão LEOC (2021) Relationship between Biomass Burning Emissions and Deforestation in Amazonia over the Last Two Decades. Forests 12(9): 1217. https://doi.org/10.3390/f12091217

Mattox GMT, Toledo-Piza M, Oyakawa OT (2006) Taxonomic Study of *Hoplias aimara* (Valenciennes, 1846) and *Hoplias macrophthalmus* (Pellegrin, 1907) (Ostariophysi, Characiformes, Erythrinidae). Copeia 2006(3): 516–528. https://doi.org/10.1643/0045-8511(2006)2006[516:TSOHAV]2.0.CO;2

Miquelarena AM (1984) Estudio comparado del esqueleto caudal en peces characoideos de la República Argentina: III. Familias Serrasalmidae, Gasteropelecidae, Erythrinidae, Anostomidae, Hemiodidae, Curimatidae y Characidiidae.

Mirande JM (2010) Phylogeny of the family Characidae (Teleostei, Characiformes): From characters to taxonomy. Neotropical Ichthyology 8(3): 385–568. https://doi.org/10.1590/S1679-62252010000300001

Oyakawa OT (2003) Erythrinidae (Trahiras). In: Checklist of the Freshwater Fishes of South and Central America. R.E. Reis, S.O. Kullander and C.J. Ferraris, Jr., Porto Alegre: EDIPUCRS, Brasil., 238–240. https://www.fishbase.se/references/FBRefSummary.php?ID=37025 [May 15, 2023]

Pires WMM, Barros MC, Fraga EC (2021) DNA Barcoding unveils cryptic lineages of *Hoplias malabaricus* from Northeastern Brazil. Brazilian Journal of Biology 81(4): 917–927. https://doi.org/10.1590/1519-6984.231598

Puillandre N, Lambert A, Brouillet S, Achaz G (2012) ABGD, Automatic Barcode Gap Discovery for primary species delimitation. Molecular Ecology 21(8): 1864–1877. https://doi.org/10.1111/j.1365-294X.2011.05239.x

Puillandre N, Brouillet S, Achaz G (2021) ASAP: Assemble species by automatic partitioning. Molecular Ecology Resources 21(2): 609–620. https://doi.org/10.1111/1755-0998.13281

Ratnasingham S, Hebert PDN (2007) bold: The Barcode of Life Data System (http://www.barcodinglife.org). Molecular Ecology Notes 7(3): 355–364. https://doi.org/10.1111/j.1471-8286.2007.01678.x

Ratnasingham S, Hebert PDN (2013) A DNA-Based Registry for All Animal Species: The Barcode Index Number (BIN) System. PLoS ONE 8(7): e66213. https://doi.org/10.1371/journal.pone.0066213

Roberts TR (1969) Osteology and relationships of characoid fishes, particularly the genera *Hepsetus*, *Salminus*, *Hoplias*, *Ctenolucius*, and *Acestrorhynchus*.

Rosso JJ, Mabragaña E, González Castro M, Díaz de Astarloa JM (2012) DNA barcoding Neotropical fishes: Recent advances from the Pampa Plain, Argentina. Molecular Ecology Resources 12(6): 999–1011. https://doi.org/10.1111/1755-0998.12010

Rosso JJ, Mabragaña E, González Castro M, Delpiani SM, Avigliano E, Schenone NF, Díaz de Astarloa JM (2016) A new species of the *Hoplias malabaricus* species complex (Characiformes, Erythrinidae) from the La Plata River basin. Cybium 20(3): 199–208. https://ri.conicet.gov.ar/handle/11336/53902 [May 15, 2023]

Rosso J, González-Castro M, Bogan S, Cardoso Y, Mabragaña E, Delpiani M, Diaz de Astarloa J (2018) Integrative taxonomy reveals a new species of the *Hoplias malabaricus* species complex (Teleostei, Erythrinidae). Ichthyological Exploration of Freshwaters 28(3): 235–252. https://doi.org/10.23788/IEF-1076

Salomón R, Melo S, Winzer N (2004) MULTIVARIADO software.

Santos JP, Guimarães EC, Garciov-Filho EB, de Brito PS, Corrêa Lopes DF, Andrade MC, Ottoni FP, da Silva Dias LJB, dos Anjos MR, Carvalho-Neta RNF, Rodrigues LRR Nogueira MAM de P, Pelicice FM, Agostinho AA, Fearnside PM (2023) Fisheries monitoring in Brazil: How can the 2030 agenda be met without fisheries statistics? Biota Neotropica 23: e20221439. https://doi.org/10.1590/1676-0611-BN-2022-1439

Santos CR, Oda-Souza M, de Almeida Jr EB, Zickel CS (2024) Effects of urban ecosystem under the diversity and structure of two forest ecotones in Maranhão state. Urban Ecosystems 27(2): 399–416. https://doi.org/10.1007/s11252-023-01449-2

Tamura K, Stecher G, Kumar S (2021) MEGA11: Molecular Evolutionary Genetics Analysis Version 11. In: Battistuzzi FU (Ed.) Molecular Biology and Evolution 38: 3022–3027. https://doi.org/10.1093/molbev/msab120

Thompson JD, Higgins DG, Gibson TJ (1994) CLUSTAL W: Improving the sensitivity of progressive multiple sequence alignment through sequence weighting, position-specific gap penalties and weight matrix choice. Nucleic Acids Research 22(22): 4673–4680. https://doi.org/10.1093/nar/22.22.4673

Toledo-Piza M, Baena EG, Dagosta FCP, Menezes NA, Ândrade M, Benini RC, Bertaco VA, Birindelli JLO, Boden G, Buckup PA, Camelier P, Carvalho FR, Castro RMC, Chuctaya J, Decru E, Derijst E, Dillman CB, Ferreira KM, Merxem DG, Giovannetti V, Hirschmann A, Jégu M, Jerep FC, Langeani F, Lima FCT, Lucena CAS, Lucena ZMS, Malabarba LR, Malabarba MCSL, Marinho MMF, Mathubara K, Mattox GMT, Melo BF, Moelants T, Moreira CR, Musschoot T, Netto-Ferreira AL, Ota RP T. Oyakawa O, Pavanelli CS, Reis RE, Santos O, Serra JP, Silva GSC, Silva-Oliveira C, Souza-Lima R, Vari RP, Zanata AM (2024) Checklist of the species of the Order Characiformes (Teleostei, Ostariophysi). Neotropical Ichthyology 22(1): e230086. https://doi.org/10.1590/1982-0224-2023-0086

Vari RP (1995) The neotropical fish family Ctenoluciidae (Teleostei: Ostariophysi: Characiformes): supra and intrafamilial phylogenetic relationships, with a revisionary study. Smithsonian Contributions to Zoology 564: 1–97. https://doi.org/10.5479/si.00810282.564

Vitorino CA, Oliveira RCC, Margarido VP, Venere PC (2015) Genetic diversity of *Arapaima gigas* (Schinz, 1822) (Osteoglossiformes, Arapaimidae) in the Araguaia-Tocantins basin estimated by ISSR marker. Neotropical Ichthyology 13(3): 557–568. https://doi.org/10.1590/1982-0224-20150037

Ward RD, Zemlak TS, Innes BH, Last PR, Hebert PDN (2005) DNA barcoding Australia's fish species. Philosophical Transactions of the Royal Society of London. Series B, Biological Sciences 360(1462): 1847–1857. https://doi.org/10.1098/rstb.2005.1716

Weitzman SH (1964) Osteology and relationships of South American characid fishes of subfamilies Lebiasininae and Erythrininae with special reference to subtribe Nannostomina. Proceedings of the United States National Museum. https://doi.org/10.5479/si.00963801.116-3499.127 [March 17, 2025]

Zanata AM, Vari RP (2005) The family Alestidae (Ostariophysi, Characiformes): A phylogenetic analysis of a trans-Atlantic clade. Zoological Journal of the Linnean Society 145(1): 1–144. https://doi.org/10.1111/j.1096-3642.2005.00183.x

Supplementary material 1

Specimens and DNA sequence data used in molecular analyses

Authors: Karen L. A. Guimarães, Juan J. Rosso, Mariano González-Castro, Sarah J. do Nascimento Andrade, Pâmella S. Brito, Erick C. Guimarães, Juan M. Díaz de Astarloa, Luís R. R. Rodrigues

Data type: xlsx

Explanation note: Detailed list of tissue samples collected for molecular analyses, including specimen voucher information for *H. maranhensis*, and accession data for comparative sequences of *Hoplias* species downloaded from BOLD.

Copyright notice: This dataset is made available under the Open Database License (http://opendatacommons.org/licenses/odbl/1.0/). The Open Database License (ODbL) is a license agreement intended to allow users to freely share, modify, and use this Dataset while maintaining this same freedom for others, provided that the original source and author(s) are credited.

Link: https://doi.org/10.3897/zse.101.155287.suppl1